UNIVERSITY OF OKLAHOMA

GRADUATE COLLEGE

SYNTHESIS, ADDITIVE MANUFACTURING, AND MECHANICAL EVALUATION OF CO-POLYMERS FOR DENTAL APPLICATIONS

A THESIS

SUBMITTED TO THE GRADUATE FACULTY

in partial fulfillment of the requirements for the

Degree of

MASTER OF SCIENCE

By PETER VU

Norman, Oklahoma

2026

SYNTHESIS, ADDITIVE MANUFACTURING, AND MECHANICAL EVALUATION OF CO-POLYMERS FOR DENTAL APPLICATIONS

A THESIS APPROVED FOR THE

SCHOOL OF AEROSPACE AND MECHANICAL ENGINEERING

BY THE COMMITTEE CONSISTING OF

Dr. Yingtao Liu, Chair

Dr. John Klier

Dr. Hanping Ding

Acknowledgement

First and most importantly, I'd like to dedicate my gratitude towards Dr. Yingtao Liu for his continuous support, dedication, and patience to me and other SMIS lab students over the years. Without him this thesis would not be possible.

I'd also like to dedicate my thanks to Dr. Chris Billings, Dr. Benjamin D. Bevans, Dr. Alexander R. Riensche for accommodating me into their very busy tensile testing schedule; Joshual Hall and Sean K. Brownlee for their guidance on using the Instron tensile testing machine; Benjamin D. Sherwood for his help on operating on some of the testing equipment, and everyone else at the Sooner Advance Manufacturing Lab for their generous accommodation and assistance.

I'd also like to thank Dr. Novruz G. Akhmedov for his catch-up chemistry lessons and his guidance on operating the NMR Spectrometer, Dr. Onkar Singh for his help with the chemical reactor, and Elijah Personette for teaching and helping me with the manufacturing work.

Last but not least, I'd like to thank Dr. John Klier and Dr. Hanping Ding for lending their time and expertise as members of my thesis committee.

Table of Contents

List of Tables

List of Figures

Abstract

3D printing has many potentials due to its ability to manufacture complex shapes as well as being very customizable. This technology is not very widespread and has only reached its infancy in dentistry. Implementing 3D printing in dentistry would allow the creation of more complex and customized dental prosthesis.

This thesis presents an in-depth investigation into the synthesis and development of a 3D-printable EGDMA-based resin formulated to cure efficiently under UV light, enabling compatibility with most commercial resin-based additive manufacturing systems. The work examines the full resin formulation process, beginning with the selection and evaluation of appropriate photo-initiators to ensure proper polymerization behavior during printing. In addition, major focus is placed on the synthesis of the resin's filler material. The filler material consists of PMMA-based copolymers synthesized with varying monomer ratios of MMA, MAA and GMA. By systematically adjusting these ratios, the study aims to understand how compositional differences influence the resulting material's mechanical performance.

Tensile testing shows that higher molecular weight copolymer improves the Modulus of Elasticity as well as UTS of the composite. The addition of GMA shows mixed results, with batch B2G, having 0.4 MAA:MMA ratio showing the best improvement in term of mechanical properties. The addition of GMA shows a 45% increase in Young's Modulus, 66% increase in Yield Strength, and 49% increase in Ultimate Tensile Strength for B2G specifically.

Chap 1: Introduction

1.1 A look into dentistry

Dentistry has been a continuous field of development for a long time in history. Early forms of restorative went back as long as 6500 years ago where Neolithic humans used bees wax as a form of tooth filling [1]. George Washington, the founding father of the U.S, is known to have very bad teeth, which were replaced with dentures made out of ivory and a combination of different alloys [2]. As technology and material science improve, so is the development of many more advanced materials that are created specifically for use in the dentistry industry.

Many different types of materials are used for dental purposes. Metals and alloys are the most prominent before the development of more aesthetically matching materials. Metals are, however, prone to tarnishing and corrosion under the typical oral condition. Because of that, only specific noble metals and metal alloys are selected to be used as teeth prosthetic. These specific alloy requirements further increase the cost, along with consumer demand for more aesthetically pleasing alternatives, making them not as popular today as other materials.

Ceramics is a more popular alternative to metal. Dental ceramics are made up of silicate glasses, porcelain, glass ceramics, or highly crystalline solids. They are a popular choice for their biocompatibility, aesthetic, high hardness, low to moderate fracture toughness, excellent wear resistance, and chemical inertness. Dental ceramics also have a lower harness compared to teeth enamel to prevent damage to the opposing and surrounding teeth. Despite many upsides to this material, there is a significant

drawback: its susceptibility to tensile fracture, especially when tensile stress occurs over defects and its inability to prevent crack propagation. Overall high brittleness and low fracture resistance are the primary drawbacks of this material.

This leaves a very popular alternative which is polymer. With its high availability and ease of use, it is becoming increasingly popular as a primary choice of dental material, capable of covering a wide range of usage.

Depending on their purposes, these materials are divided into three categories: auxiliary, preventative, and restorative use. Auxiliary materials are not applied on the dental structure itself but instead used to construct dental tools, prostheses, and appliances. These include impression materials, cast materials, teeth aligners, polishing abrasives, etc. Due to its high adaptability, polymers are very often used as an auxiliary material. Preventative materials are used to prohibit the development of tooth decay as well as to seal and prevent leakage from the tooth. These are typically used due to their antibacterial properties, protecting the tooth from further bacterial damage. Last are restorative materials, which are used to either partially or fully reconstruct the teeth structure. These can be divided into three subcategories, which are direct, indirect, and temporary restorative material. Direct and indirect restorative material are categorized based on whether they are used intraorally to perform restoration directly on the teeth structure or used to create prosthetics and replicas to be installed directly onto the teeth and jaw structure. Metals are often used as both direct and indirect materials because of their high durability and strength. Ceramics are implemented as an indirect restorative material through traditional subtractive manufacturing, as well as being used as a direct

restorative material by implementing it as a component of a composite resin for both direct and indirect restoration [3], [4].

1.2 Polymer review

The successful integration of polymers into dental applications is largely attributed to their highly tunable mechanical, chemical, and biological properties. Understanding the evolution of dental materials provides context for modern polymer-based restorative systems.

A polymer is a molecule compromised of long sequences of repeating structures called monomers, linked together by primarily covalent bonds. The act of creating a macromolecule through linking monomers together using chemical reaction is called polymerization. The connecting monomers could result in many different structures depending on how they connect, with each of those structures alternating the physical properties of the polymer. These monomer units can connect in either forms of a chain, loop, branch, or network, result in different structures, shown in Figure 1.

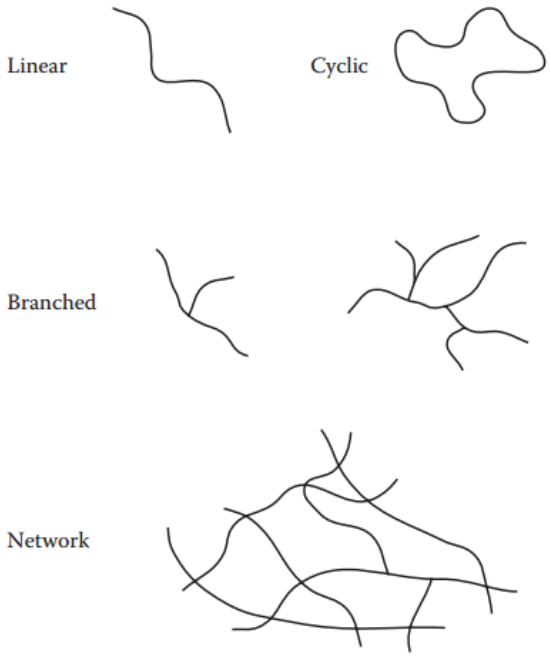

Figure 1: Different polymer structures [5]

Polymerization can occur in two different ways, either through radical or ionic polymerization. Both radical and ionic polymerization contain three stages: initiation, propagation, and termination. Radical polymerization is the chain growth process involving free radical, or molecule that contains an unpaired electron. The initiation stage starts with an initiator molecule, which breaks down into a radical. This free radical would attach to a monomer, forming a radical chain that attracts and attaches to more monomers in the propagation stage. The radical chain will keep growing until it attaches to another radical chain, which results in the full formation of the polymer, causing chain termination. Ionic polymer also involves the use of an initiator. During the initiation process, the initiator molecule first reacts with a monomer to create an initiator-monomer adduct. This bigger molecule carries a charge on the monomer end,

which reacts with another monomer to form a bigger adduct with a charged end, hence the process keeps on repeating, resulting in the propagation process. Statistical collisions allow the growing anionic chain to react with monomers, which keeps the process repeating until there are no available monomers left to react with. Radical polymerization is used more due to its higher compatibility with most monomers and its faster reaction rate but is very susceptible to inhibition by moisture and oxygen. Ionic polymerization, in return, sees more limited use due to its low compatibility with most monomers as well as its lower tolerance for impurities, but offers better control over molecular weight as well as the polymer architecture.

After formation, chain and branch polymer that grew beyond their entanglement length are usually tangled and intertwined together, held together by the weaker van de Waals' force. This structure, therefore, can be melted and experience glass transition state when heated up to certain temperatures. This is classified as thermoplastics. Unlike linear and branch polymer, in network polymers, these molecules are connected at multiple sites, via the stronger aforementioned covalent bonds. These are classified as thermosets because they undergo an irreversible setting process during polymerization [6].

To get different properties from different polymers, their equivalent monomers are mixed to synthesize a different type of polymer. These are called copolymers, which contain at least two different types of monomers as opposed to homopolymer, which only contain one singular type of monomer. This is done as opposed to mixing two different polymers together because generally, different polymers are immiscible. The

order that these monomers connect can be in an alternating manner, or entire random, as shown in Figure 2.

~A-A-A-A-A-A-A-A-A-A-A-A-A-A-A-A-A-A-A-A-A-A-A-A-A-A~

Homopolymer

~A-B-A-B-A-B-A-B-A-B-A-B-A-B-A-B-A-B-A-B-A-B- A-B-A~

Alternating copolymer

~A-B-A-A-A-B-B-A-B-A-A-B-B-B-B-A-B-A-A-A-B-B-A~

Random copolymer

Figure 2: Comparison between homopolymer and different types of copolymers

Within dentistry, different manufacturing methods are used depending on each type of material used. For direct restoration, resin-based composite is typically used. Dental resin composite contains three main elements: the cross-linking monomer matrix, an initiator, and a filler element. The filler element typically is made up of small particle elements of ceramics or other materials used to enhance the mechanical properties of the matrix. The initiator is what allows the material to be used as a direct restorative material. The initiator, usually activated via UV light, is what causes polymerization on the matrix, bonding the repair material to the tooth surface. After application of the material to the tooth surface, the material is exposed to UV light, causing the monomer matrix to polymerize, trapping the filler material into the cross-linked matrix.

1.3 A look into additive manufacturing

With the advancement of additive manufacturing, also known as 3D printing, the same photo-activated resin could also be used as a form of indirect restorative material. Traditionally, dental prosthesis is made using many molding techniques, where the material is applied or injected into a mold, and then the whole assembly is exposed to either heat or microwave, depending on the material, to cure. Using molds does come with some downsides. Since the process of polymer curing is exothermic, this can cause a concentrated or uneven heat buildup within the mold. This concentration in heat causes small pockets of monomers to vaporize, leaving pores and cavities in its place. This along with the potential effect of uneven mixing of the material as well as improper filling of the mold could exacerbate the voids.

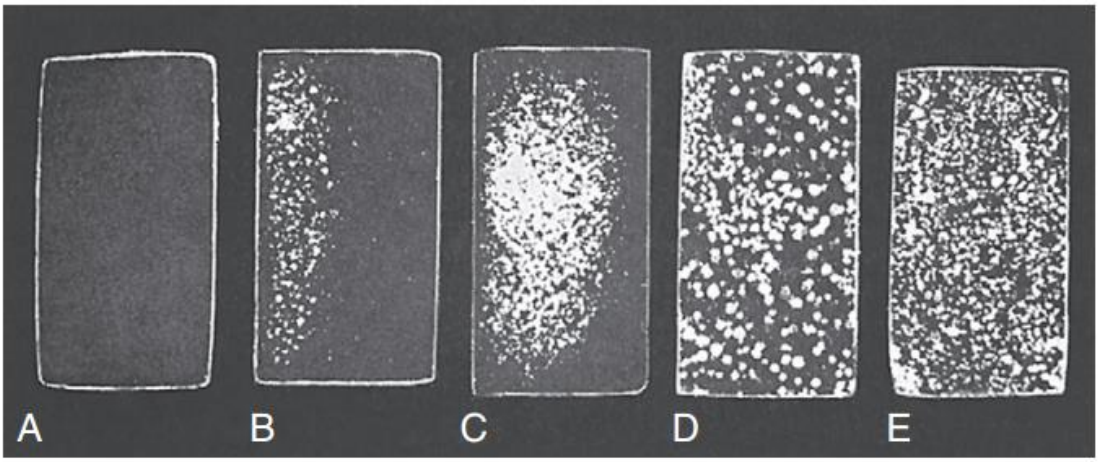

Figure 3: Heat activated resin exhibit different types and degrees of porosity: (A) properly polymerized, no porosity; (B) and (C), relatively small subsurface voids; (D) Insufficient mixing, large voids resulting from localized shrinkage. (E) Insufficient pressure during polymerization, relatively large, irregular voids. [7]

These downsides are eliminated when using 3D printing technology. In addition to this, 3D printing also allows for more variety in prosthetic designs without limitation of availability of different mold designs. Additive manufacturing is divided into different categories depending on the mechanics of material deposition. Fused Deposition Modeling (FDM) is the most common and popular form of 3D printing, but it is not used in the dentistry environment due to its relatively low precision for oral prosthesis. Instead, resin-based 3D printing is used for their high precision for small parts. Resin-based printing is divided into three different categories, which are stereolithography (SLA), masked stereolithography (MSLA), and digital light processing (DLP) printing. These printing techniques rely on the same principle: polymerizing photo-activated resin to produce working parts. The method which these printers used to cure the resin differs from each other, shown in figure 4, but the result is high accuracy, high precision small parts [8].

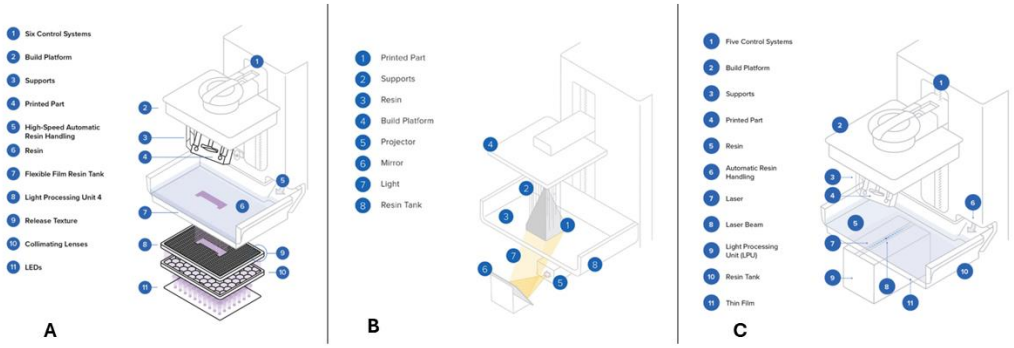

Figure 4: Difference between (A) MSLA, (B) DLP, and (C) SLA printers [8]

The makeup of the resin used for 3D printing is similar to the resin based composite material used for indirect restorative, being that it contains three primary

parts: a photoinitiation element, a highly crosslinking monomer, and a form of filler element as well as some other additives to improve other properties such as shelf stability and handling [9]. One of the most popular options for the crosslinking monomer is Ethylene Glycol Dimethacrylate (EGDMA). This monomer is picked due to its exceptional cross-linking capabilities and is an ingredient in many different dental resins. The cross-linking capability comes from the monomer having 2 double bonds, which simultaneously form polymer chains and link to other polymer chains during the free radical polymerization. Different types of radical initiators could be used to cause radical polymerization, with photoinitiator being one used because it could be activated on demand using UV light.

The filler material serves multiple purposes within the polymer mixture, but its primary purpose is to improve the mechanical properties of the crosslinking matrix. There are many different materials that can be selected, but polymer or polymer-based material is getting more popular as an option due to its highly customizable form. Poly-methyl methacrylate (PMMA) had been a very popular choice due to its biocompatibility and good mechanical properties [10]

Since filler materials significantly influence the mechanical properties of resins, modifying these materials can effectively enhance resin performance. One approach is to improve the connection between the binding material and the cross-linking matrix. In their study *Glycidyl methacrylate-modified poly(acrylic acid)*, Buzzetti et al. demonstrated that incorporating glycidyl methacrylate (GMA) into poly(acrylic acid) (PAA) polymer chain increases the binding between the EGDMA matrix and PAA polymer. The GMA connect with the PAA monomer, creating a functionalized polymer:

polymers with attached functional group giving them unique roles and properties. [11] These functionalized polymers come with pendant double bonds that when dissolved in the EGDMA monomer, polymerized the pendant double bond, attaching them to other EGDMA monomers. When the mixture is polymerized, the functional polymer with attached EGDMA would cross-link with other EGDMA monomer, incorporating the polymer “filler” into the crosslinks [12]. The process is demonstrated in the following figure:

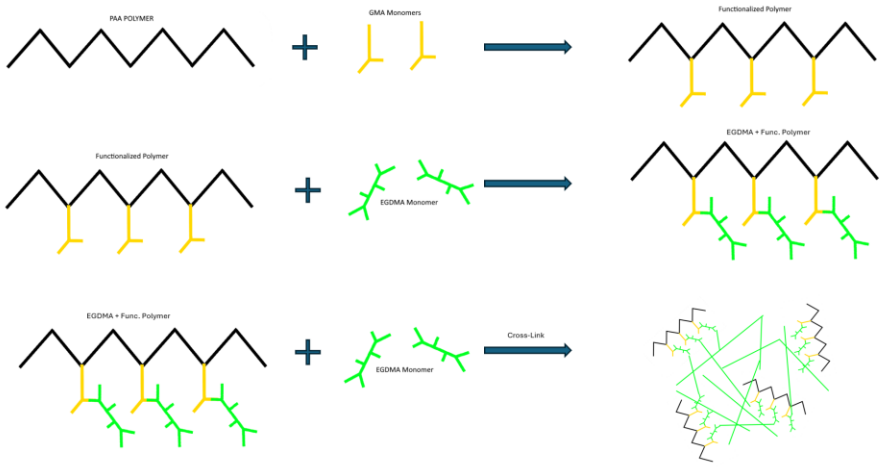

Figure 5: PAA "Filler" Modifying Process

This approach could also be applied to modify PMMA, the polymer used in dental resin impregnation, potentially resulting in enhanced mechanical performance.

1.4 Structure of thesis

This thesis intends to discuss the evolution of synthesizing an EGDMA-based resin that would polymerize under UV light exposure to be used with typical commercial 3D printers. Chapter 2 will focus on initial attempt at making an EGDMA based resin along with photoinitiator selection. Chapter 3 dives into the manufacture of the filler material along with testing how different copolymer composition would affect the nature of the material. Chapter 4 goes deep into the tensile testing process as well as result analysis. Chapter 5 will discuss the conclusion as well as potential of this material.

Chapter 2: Initial testing with EDGMA

2.1 Finding Photoinitiator

The first step is to identify what type of photo-initiator would cause the EDGMA to cure. Multiple photo-initiator candidates are tested to see their efficacy polymerize the monomer under exposure to the UV light. Three initial candidates are selected due to their wide use as a form of photoinitiator. These are Camphorquinone, Dimethylaminoethyl methacrylate, and 2-Hydroxy-4′-2-hydroxyethoxy-2-methylpropiophenone (2-Hydroxy). Camphorquinone and 2-Hydroxy showed no reaction after mixing with the EGDMA monomer and UV light exposure. Only dimethylamioethyl methacrylate (DAM) showed reaction with the EGDMA. The reaction resulted immediately after the two chemicals are mixed together, forming a soft clump. It seemed that the addition of the DAM immediately triggered premature polymerization, resulting in a stringy, soft substance even without exposing to UV light. The following figure shows the result of the two substances mixed together:

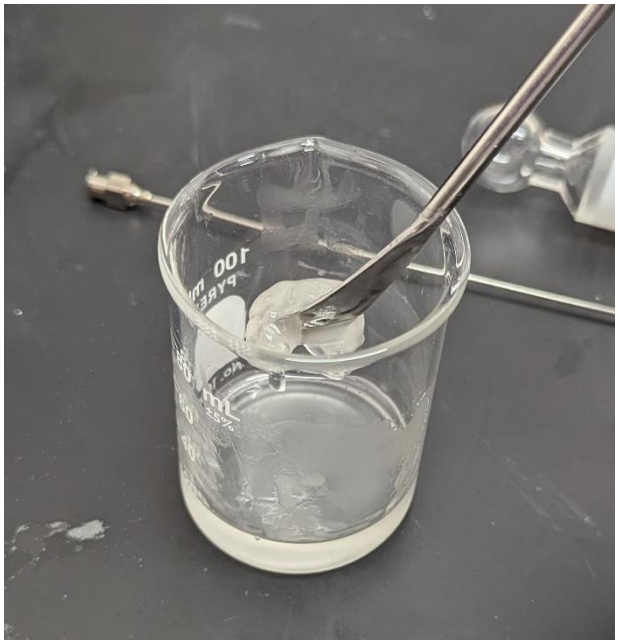

Figure 6: Result of EGDMA mixed with DAM

This behavior can be explained by DAM containing tertiary amine functional group, which is a strong electron donor. Tertiary amines are known to generate free radicals through electron-transfer interactions with oxygen or with the methacrylate carbon–carbon double bond. These radicals can initiate chain polymerization spontaneously, leading to an uncontrolled, premature curing reaction. As a result, DAM is chemically unsuitable as a photoinitiator for this resin system, along with Camphorquinone and 2-Hydroxy, which shows no reaction under UV light exposure.

Further research showed a fourth option that is often used: Diphenyl (2,4,6 trimethylbenzoyl) phosphine Oxide (DPO), which comes in as a white powder form. Initial mixing with EGDMA showed that the DPO dissolved with the EGDMA after thoroughly mixed, with no reaction shown after the solution became homogenized. The beaker is then exposed to UV light with 405mm wavelength, the solution starts to

harden. The resulting plastic is very brittle, thus proving that polymerization occurred and the photoinitiator worked.

Since polymerization had been achieved, the solution could be polymerized into dogbone samples to use as a control for tensile testing. To determine the dogbone size, the maximum depth of polymerization achieved with 405mm UV wavelength is required. To test this, a mixture of EGDMA and the photoinitiator with a ratio of 4:1 (wt/wt) EGDMA to photoinitiator is poured into a modified glass beaker. The high ratio ensures that the cross-linking of the EGDMA will be guaranteed. The beaker is covered at all sides with masking tape limiting UV light exposure to the top surface of the beaker. The beaker is then placed in the ANYCUBIC Wash & Cure Plus machine set to curing mode, which exposes UV light from the UV lighting fixture for a set amount of time. The figure below shows the testing setup:

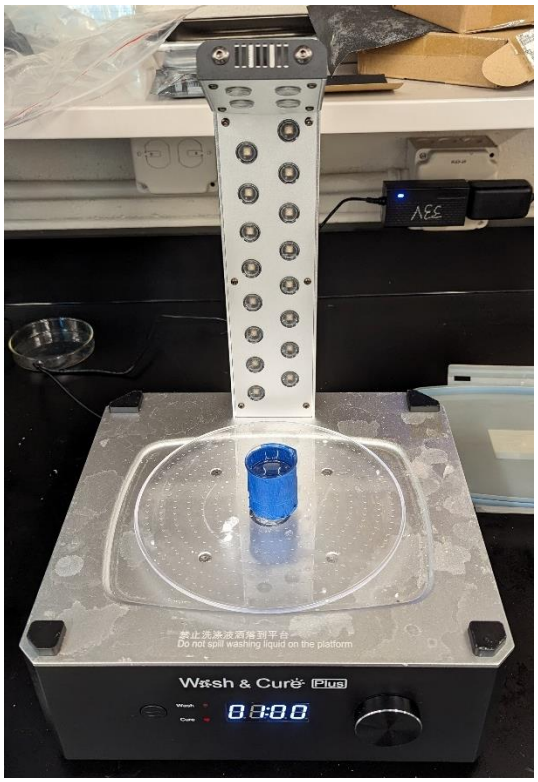

Figure 7: UV penetration testing setup

The machine is set to cure for a one-minute interval, after which the tape removed from the beaker to measure the curing depth, and reapplied after measurements are taken. The process is repeated six times. The result is shown in the figure below:

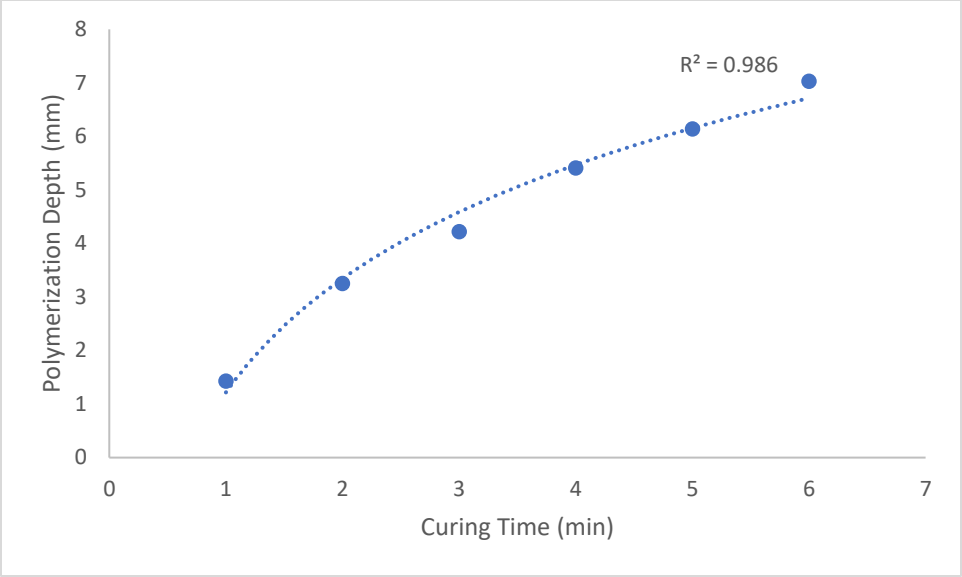

Figure 8: Curing thickness vs. Time of EGDMA

From the result, it is estimated that the max curing depth of the EGDMA is around 8mm. From this, it is determined that dogbone shape for testing purpose is ASTM D638 Type 5, with the dimensions shown in the following figure:

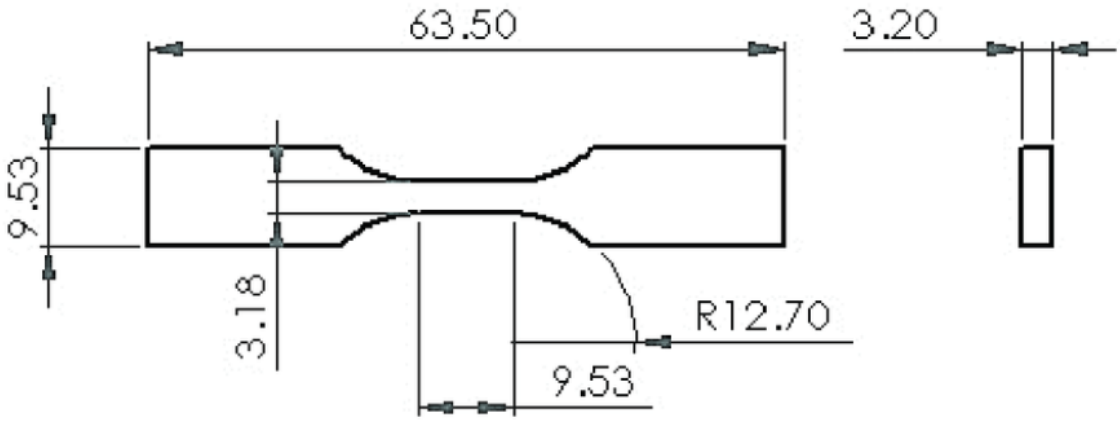

Figure 9: ASTM D638 Type 5 dogbone dimensions

The reason for selecting the specimen size is due to availability of the reverse mold as well as the curing time of each specimen only being 2 minutes, with the thickness of the sample being 3.2mm based on the data gathered in Figure 9.

The dogbone specimen will be cast using silicone molds. EcoFlex 00-30 silicone rubber is used to construct the mold from the aluminum ASTM D638 Type 5 dogbone reverse mold. Figure 10 shows both the silicone mold and aluminum reverse mold.

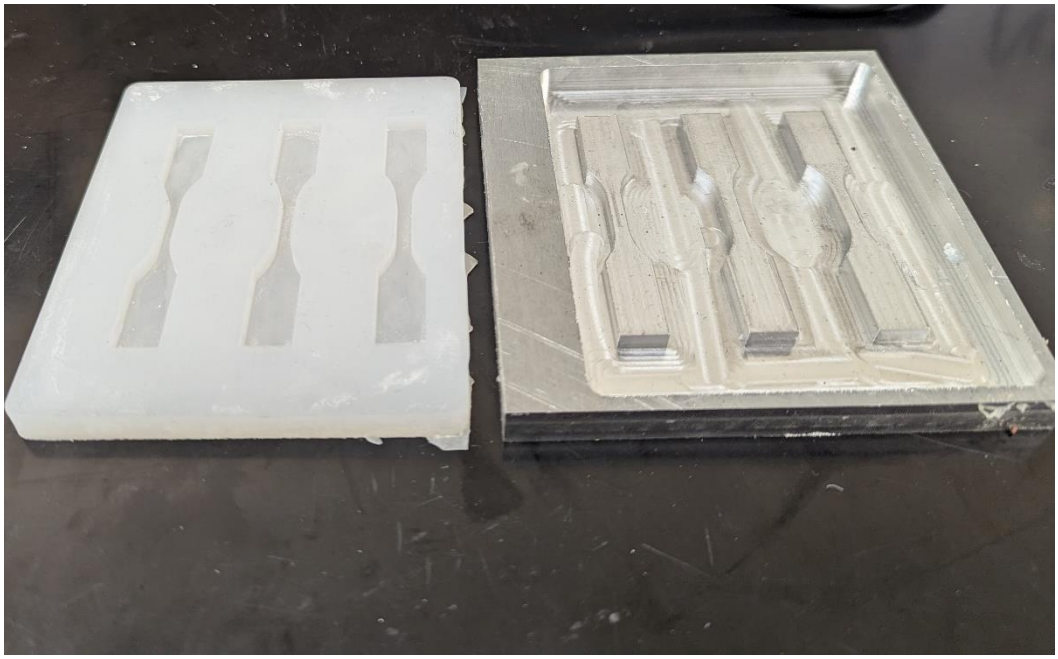

Figure 10: Silicone mold (left) and Aluminum reverse mold (right)

Initial batches of EGDMA dogbones are cast using 1% (m/m) photoinitiator concentration. After mold release is applied to the mold, the solution is poured into the mold using medical syringes to control the amount poured. After that, the mold is placed inside the Wash and Cure machine set in cured mode, with a time duration of 2 minutes. The problem occurred during the two-minute exposure to UV light, the

dogbone started to curl up as shown in Figure 11. The cast bones could not be used for tensile testing as a result.

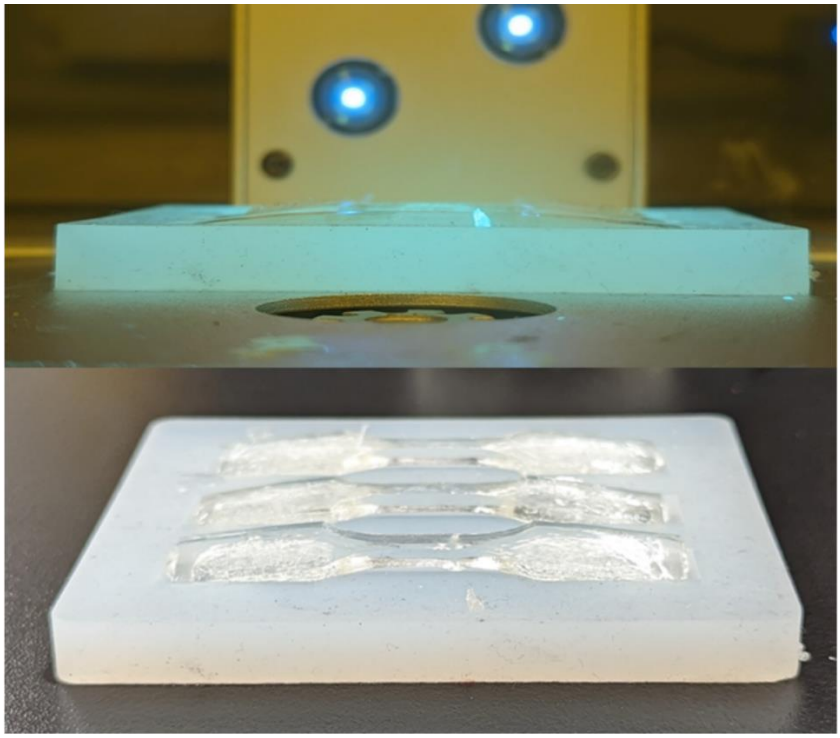

Figure 11: Dogbones being bent after being cured under UV light

In an attempt to remedy this, a transparent 4 in. x 4 in., 1mm thick acrylic sheet is placed on top of the mold before UV exposure to prevent curling from happening. This, however, resulted in the dogbone sticking to the acrylic sheet, with the curling effect still occurring, bending the acrylic sheet in the process. Attempting to remove the dogbones from the acrylic sheet results in the bone breaking, unusable for tensile tests.

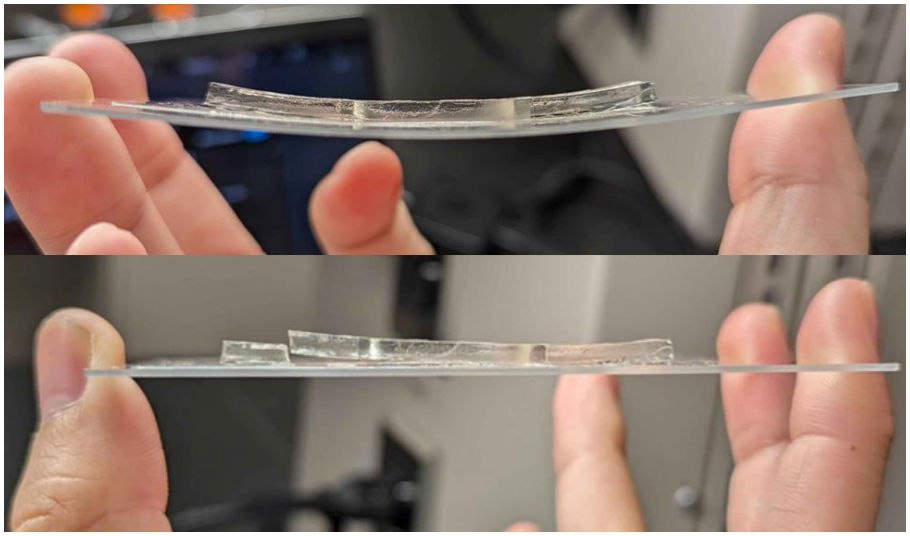

Figure 12: Curled dogbone adhere to acrylic plate

Even after mold release is applied on the acrylic sheet to prevent the sample from sticking to its surface, the curving of the sample still occurred. Thicker acrylic plates are considered to keep the dogbones flat during polymerization, but this would compress the silicone mold, altering the final thickness of the dogbone.

Looking further into the problem, the curling could be caused by internal stress developed inside the dogbone during UV exposure. Since crosslinking development of the EGDMA monomer is an exothermic process, uneven heat concentration differing by depth, which is directly caused by uninterrupted UV exposure on the top surface. Measurements taken right after dogbone formation shows that certain areas of the mold reach around 90-110°C, resulted from extreme heat build up that causes the curling.

If the UV light exposure could be altered, this would reduce the heat build-up and concentration, resulting in less internal stress development. To alter UV light exposure to the mold, the exposure time is changed from a continuous 2-minute exposure to four

30-second intervals, with 30 seconds of rest in between each interval to allow time for the cross-linker to cool down. This proved successful in creating flat dogbones, but with double the production time of each batch. Furthermore, due to the curing machine's limitation of not having a rest timer, timing had to be done by the operator.

To further reduce fabrication time, a rotating platform is placed inside the curing machine. The rotating platform, shown in Figure 13, would reduce the exposure time of the mold since the UV lighting fixture does not cover the entire platform, eliminating the need for an operator to manually pause and restart the machine.

Figure 13: Rotating Platform of the Wash & Cure machine

The resulted polymerized EGDMA dogbone is transparent with no initial deformation, shown in Figure 14. The polymerized EGDMA is very brittle and transparent when first removed from the mold.

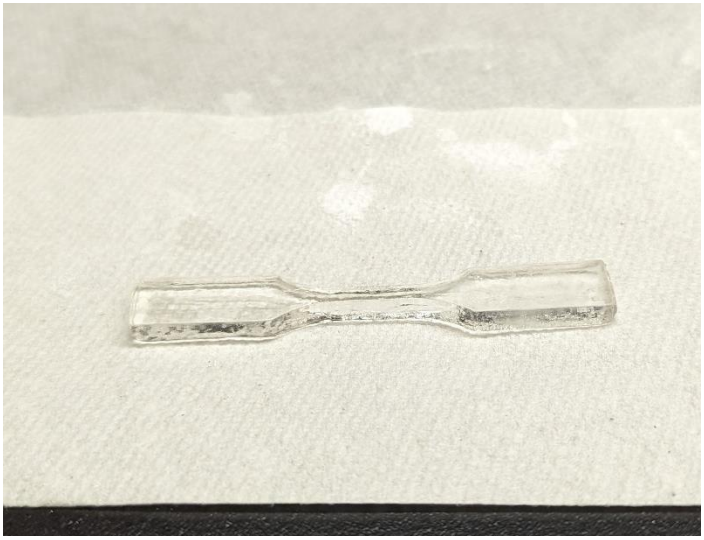

Figure 14: EGDMA Dogbone from rotating platform

One problem that was ran into was the syringes used to fill the mold up with the EGDMA starts to fail after 5 to 6 uses. It turns out that the EGDMA causes the seal between the barrel and plunger to fail, making the seal separating from the plunger and stuck in the barrel. To mitigate this, glass syringes are used as a replacement for the medical syringes used before. These syringes come with Luer-lock thread that allows a more secure connection with different tips, which allows more control of fluid flow out of the syringe. Figure 15 shows the new glass syringes.

Figure 15: Glass syringes with Luer-lock head

2.2 Identify photoinitiator concentration

When the dogbone sample cools down, cracks and voids start to develop, weakening the sample to the point of invalidating it from being used for tensile testing. To test the correlation between photoinitiator concentration and void development, three different batches of EGDMA and photoinitiator mixture, each being 2%, 5%, and 10% photoinitiator concentration are created. Twenty samples are created from each batch, using the same method of dogbone fabrication as mentioned above. The table below shows the failure rate of each batch.

Table 1: Failure rate of different photoinitiator concentration

Photoinitiator Concentration (wt/wt)	Samples Created	Samples Failed	Failure Rate
2%	20	19	95%
5%	20	12	60%
10%	20	5	20%

Based on the collected data, the photoinitiator concentration does correlate with the failure rate of the sample, higher concentration lowering the likelihood of the sample failing during cooling. Failure ranges from cracks and void developing within the sample to the sample completely breaking apart, shown in the following figure.

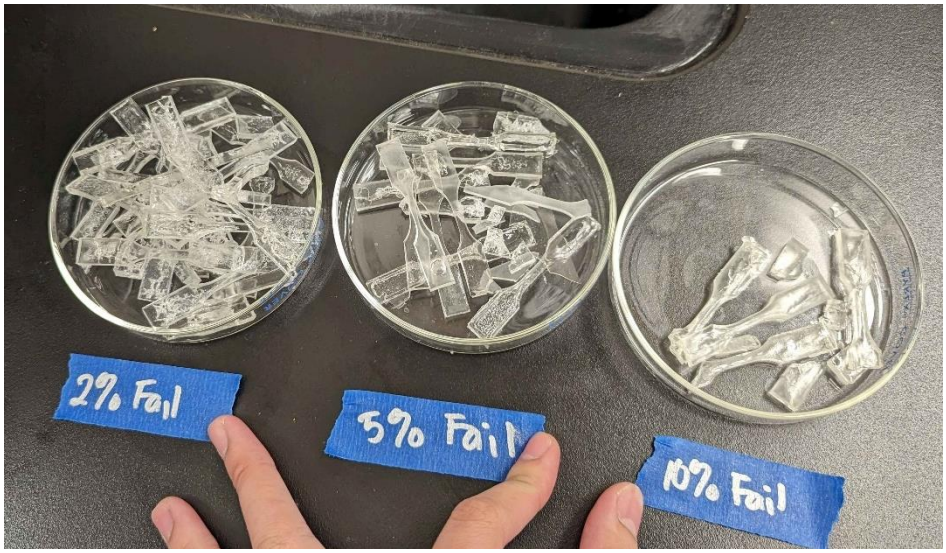

Figure 16: Failed sample of different photoinitiator concentrations

Despite the correlation, having higher photoinitiator concentrations is not the correct method of addressing the problem. Most photoinitiator system used in dental

polymer generally has a concentration of less than 2%, and going beyond 5% does not provide any additional benefits to the properties of the photocured polymer [13], [14]. Further research shows that photoinitiator polymer systems generally requires a polymer serving as a "filling material". The excess of photoinitiator in higher concentration batches serves as a "filling material" for the cured crosslinker, reducing its chance of developing cracks and internal void when cooled down.

After further literature review, the article "Development of Dental Poly(methyl methacrylate)-Based Resin for Stereolithography Additive Manufacturing" by Hata et. al, the results seem to align with the findings. According to the article, when attempting to print with resin with very high ratio of EGDMA, the printed model developed internal cracks and is classified as a failed print. The use of cross-linkers without polymer filling will result in the cured product developing failures and internal cracks, rendering it inoperable [15]. Due to this, to achieve successful samples, additional polymer must be incorporated into the EGDMA mixture. Pure EGDMA and photoinitiator could not be used as a control group for future mechanical testing.

Chapter 3: Synthesis of PMMA

Polymethyl methacrylate (PMMA) is a polymer made from Methyl methacrylate monomer (MMA). Synthesizing the polymer requires the use of an initiator, which serves as the molecule that kickstarts polymerization. For PMMA, azobisisobutyronitrile (AIBN) is used as an initiator. PMMA is chosen as the first polymer to be synthesized due to it being very similar to the target polymer, PMMA-co-MAA, only having one extra ingredient, methacrylic acid (MAA) compared to PMMA. This initial round of synthesizing will serve as a learning platform for future polymer synthesis.

3.1 Reaction Chamber Configuration

All the synthesis of the polymer is performed in a glass reactor. The glass reactor is obtained from Ace glassware as an all-in-one bundle with product number 6542-12. This includes major components such as the reactor chamber, heating mantle, and a stirring assembly with variable speed motor controller, stirring rods with paddles. Due to the need to use solvent that releases toxic fumes, all synthesis operations are performed inside a fume hood. The following figure shows the reactor fully assembled. Table 2 shows the list of components of the reactor.

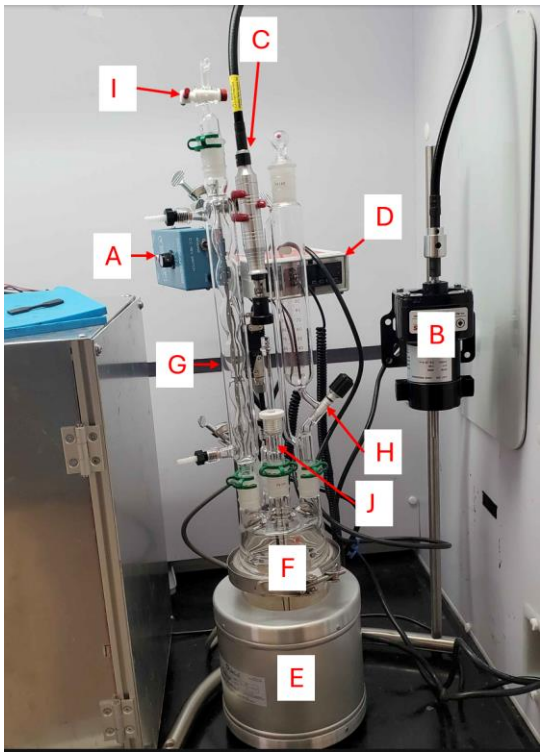

Figure 17: Ace Glassware Reactor

Table 2 List of items in Reactor package

Label	Name	Function
A	Motor Speed Controller	Control speed of motor
B	Stirring Motor	Provide power to stir rod
C	Flexible Coupling connected to Stir rod	Transfer power from motor to stir rod
D	Temperature Controller	Control the heat output of heating mantle
E	Heating Mantle	Provide heat to the chamber
F	Reaction Chamber	Where chemical reaction takes place
G	Condenser	Condense solvent for reuse
H	Pressure Equalizing Graduated Funnel	Allow addition of chemicals at controlled rate
I	Right angle Hose adapter with valve	Allow air inlet
J	Stirrer Bearing	Allow Stirring Shaft to pass through while keeping chamber airtight

3.2 Initial PMMA Synthesis attempt

PMMA polymer synthesis is performed using menthyl methacrylate (MMA) monomers with 2,2'-Azobis(isobutyronitrile) (AIBN) used as an initiator. Both solutions are added into the reaction chamber along with a large amount of toluene used as a solvent. The ratio of monomer to solvent is generally recommended at 10:1 so it is mixed this way for the reaction. When initially mixed, the solution is clear and pertains no color. The chamber temperature is set at 70°C and the solution is mixed constantly at this temperature for 2 hours. While mixing, Argon gas is constantly fed into the

chamber, ensuring that there is no moisture or oxygen inside affecting polymerization. Keeping the environment inside the reactor free of oxygen and moisture is paramount due to oxygen being an inhibitor that would terminate polymer chains. After two hours, the mixture remained to be a homogenous solution still with a clear color, indicating that the polymer is still fully dissolved in the toluene.

To separate the polymer from the solvent, the solution is poured into hexane. The solution is separated and the polymer condensation forms at the bottom of the hexane bath, as shown in Figure 18

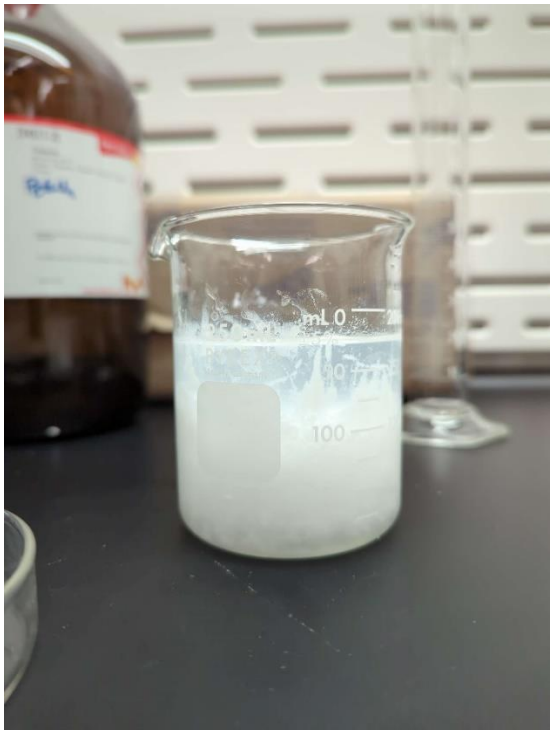

Figure 18: PMMA solution separated and condensate at the bottom of hexane bath

The entire hexane solution is then poured through a filter, with the solid part collected and heated in an oven at 50℃ until dried. The following image shows the result of dried polymer:

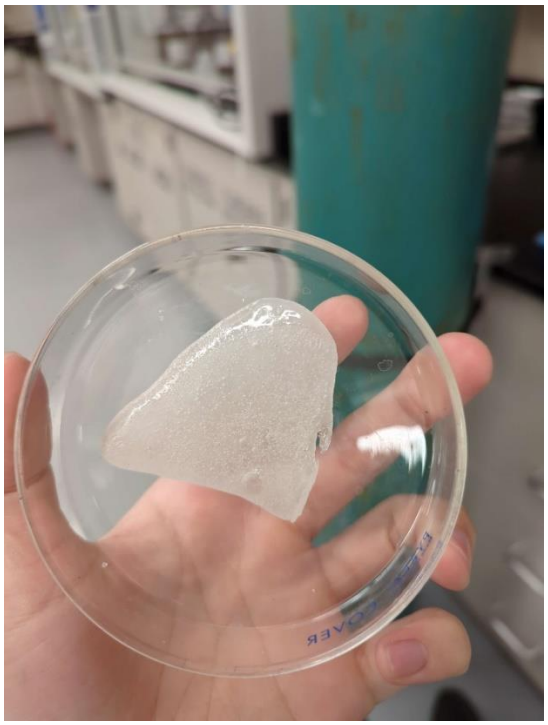

Figure 19: Dried PMMA Polymer

3.3 Reaction Chamber Improvements

The initial setup of the reactor chamber is not very optimized as it comes with two major issues: difficulty adding chemicals into the reactor, and hard to identify the argon gas flow.

The graduated funnel comes with a flow rate adjustment knob, which allows the operator to adjust the rate at which chemicals are added as well as graduation, which the operator can roughly measure how much chemical is added before dropping the chemical into the chamber. Due to the extended height of the graduated funnel, as well as the fume hood limiting how high the hood door could be raised, the process of adding chemicals into the reactor becomes unnecessarily difficult. The operator had to pour chemicals into the reactor at an awkward position, often resulting in the chemicals not

making it into the reactor. Considering that the reactor only had to be air-tight but not pressurized, as well as the chemicals not needed to be added in at a controlled rate but added all at once at the beginning, the graduated funnel is replaced with a goose-neck adapter that is short enough to not require the operator to reach for the entrance as well as allowing the use of a typical glass funnel without the funnel being in the way of other components to simplify the chemical adding process. After the chemicals are added, the funnel is replaced with a glass cork to reseal the reaction chamber.

Since it is paramount to ensure that no moisture made it into the chamber during synthesis, Argon gas is used to feed into the chamber. The initial layout of the reactor only allowed air to be supplied into the chamber but not removed from it. Without continuous air flow through the chamber, any moisture and oxygen that was initially inside the chamber would not be purged from the chamber but only be displaced. This would negatively affect the chemical reaction. A simple solution would be to remove one of the glass corks to allow air flow, but this is not a reliable solution. If Argon supply got interrupted, outside air would simply get inside the chamber through the opening. To mitigate this, the opening slot is connected to a right-angle adapter that is connected to a bubbler. The bubbler serves both as an indicator of the flow of the Argon gas as well as a check valve preventing outside air from flowing back in case the Argon flow got interrupted, ensuring no outside oxygen and moisture can get back inside the chamber. In addition to the bubbler, the old stirrer bearing is replaced with a new one that allows a gas inlet, which is used to free up the top inlet ports. The following image shows the updated reactor setup.

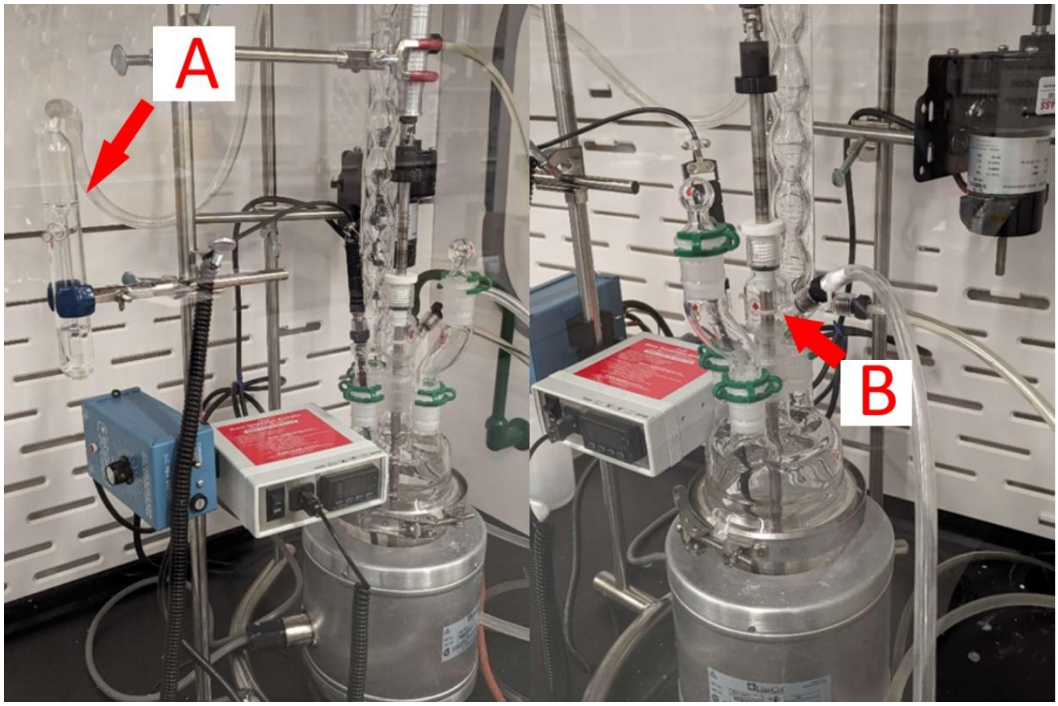

Figure 20: Changes to the reactor setup: A) Added bubbler; B) New Stirrer Bearing

3.4 PMMA-co-MAA synthesis

The process of creating PMMA-co-MAA polymer is very similar to the PMMA synthesis. During the initial phase of adding all the chemical components, methacrylic acid (MAA) is added on top of the MMA as well as the initiator. Mixing time and temperature remained the same as the PMMA synthesis process. Since both the MMA and MAA monomers are added at the same time at the beginning, as well as the solution being constantly and evenly mixed during the reaction period, the resulted copolymer should have a random and even distribution between the MMA and MAA monomers.

After the two-hour synthesis period, the product came out differently compared to the PMMA solution. The mixture has a white opaque color, with a consistency similar to a very thin slime sludge. After 5 minutes of being undisturbed, the solution starts to

split, creating a clear boundary. The following image shows the solution right after retrieval from the reactor as well as the polymer separating from the solvent after leaving undisturbed for a period of 5 hours (the extra toluene is extracted to speed up the drying process).

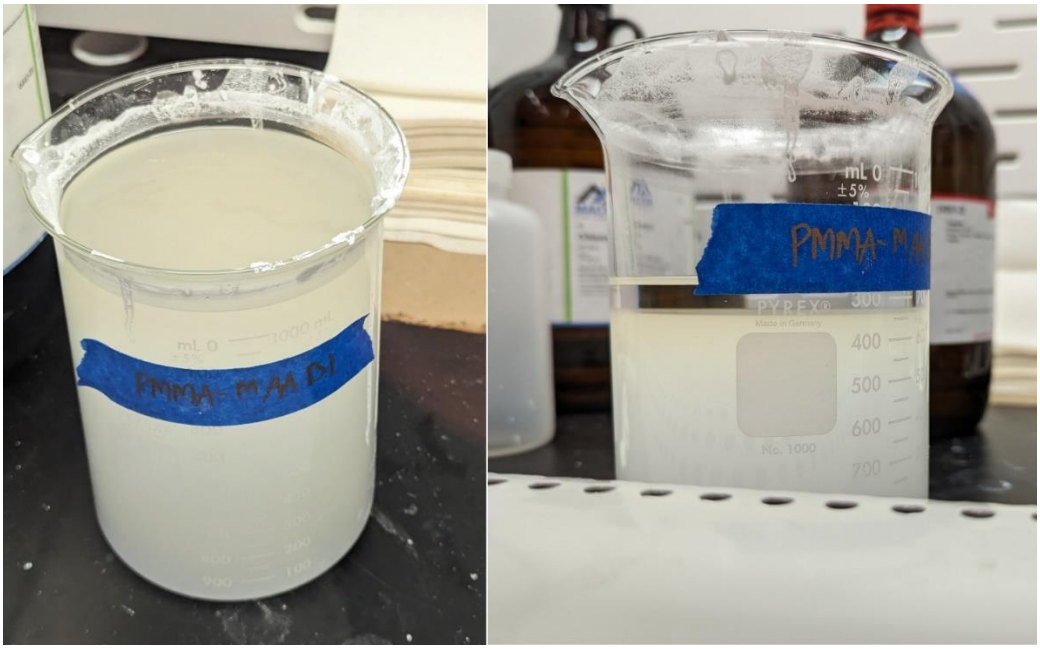

Figure 21: PMMA-co-MAA polymer diluted in toulene

Due to the ease in separation between the polymer and the solvent, the mixture is simply left inside the fume hood for the toluene to evaporate, drying out the polymer. The drying process takes around 2 days but could be sped up using an oven. The final dried copolymer product can be seen in the figure below:

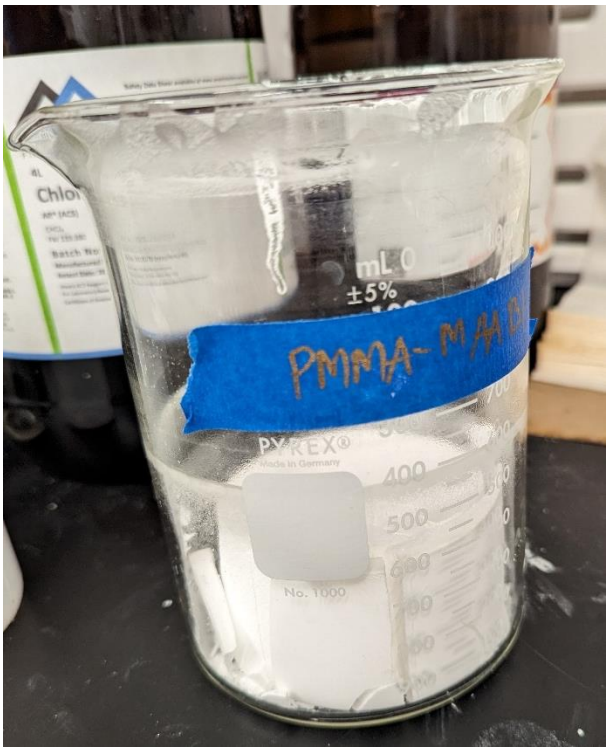

Figure 22: Dried PMMA-co-MAA polymer

3.5 Mixing EGDMA and PMMA-co-MAA

To add the copolymer to the EGDMA, the copolymer first needs to be broken down into powder form. This is achieved by using a mortar and pestle to crush the copolymer. The copolymer is then added to the EGDMA and photoinitiator mixture with 10% (wt-wt) concentration and stirred together. However, after mixing, the solution starts to split with the copolymer concentration at the bottom of the vessel after about 1 minute, shown in Figure 23, not leaving enough time for tensile dogbone fabrication.

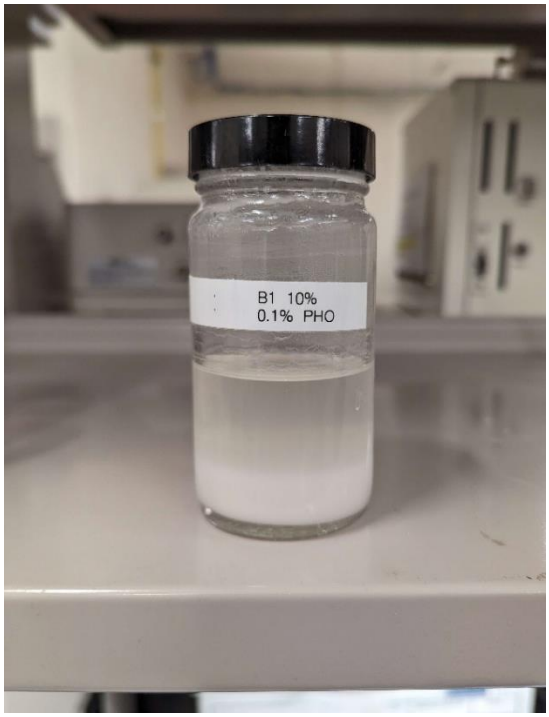

Figure 23: Photopolymer solution splitting after mixed

More vigorous stirring by hand is attempted but the result still remains the same. To remedy this, the solution is instead mixed using a sonicator as shown in Figure 24. Different timings are tested, and 30 seconds gives the best balance between the solution being thoroughly homogenized and not being too hot.

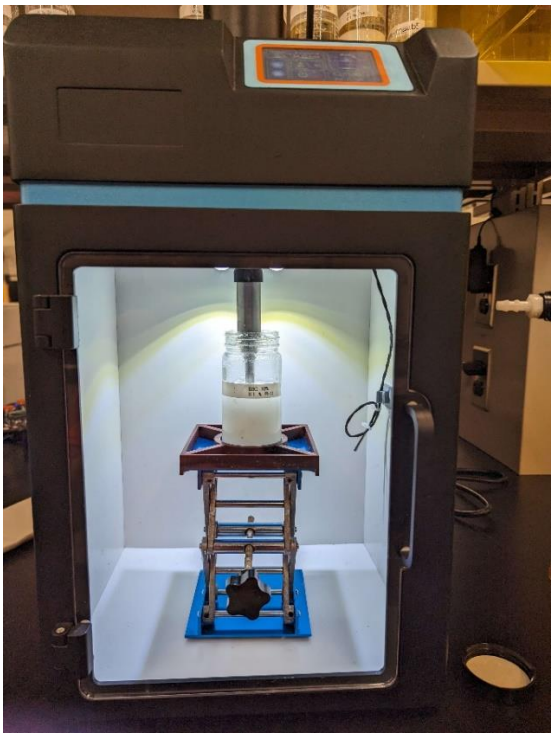

Figure 24: Monomer solution homogenized using the sonicator

When further tested, it is found out that four minutes is the limit before enough heat is introduced into the solution, activating the EGDMA and starting the cross-linking process. This resulted in the solution being solidified into a mush-like substance, becoming unworkable, as shown in Figure 25. Temperature measured immediately afterwards shown to be 92 ℃.

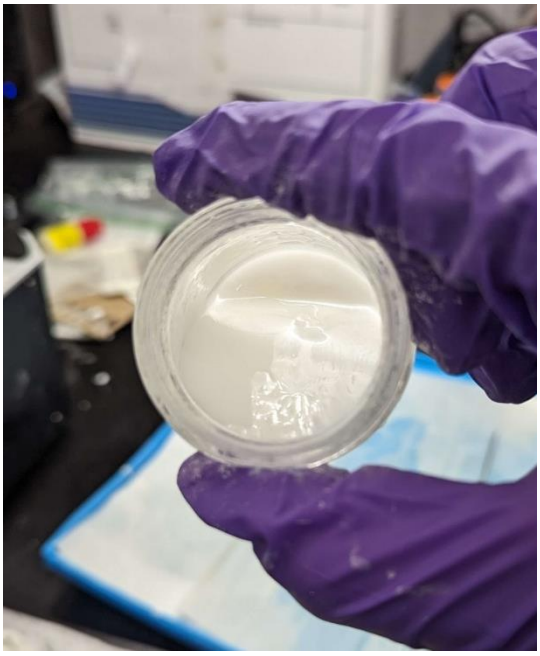

Figure 25: EGDMA solution activating due to excessive heat introduced by the sonicator

The vibration produced by the sonicator causes the mixture holding vessel to shift around, potentially damaging the vessel itself. To remedy that, a simple adapter is created to stop the container from moving around, as shown in Figure 26.

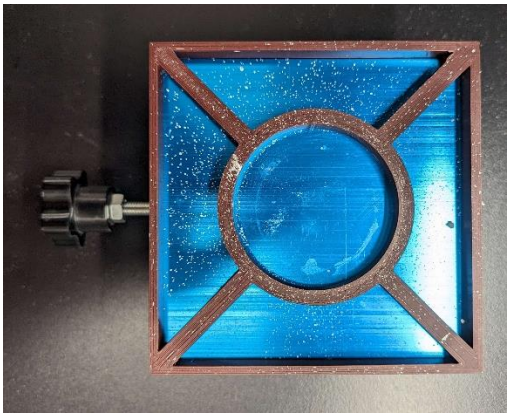

Figure 26: Adapter attached to vessel stand

The same dogbone manufacturing process from above is repeated with the new homogenized monomer solution: the solution is filled to the top of the dogbone silicone mold to prevent capillary action from affecting the geometry of the bone. The mold is then placed on the rotating platform of the curing machine where it is cured for two minutes. The sample came out very stable and did not develop cracks after cooling down, as shown in Figure 27.

Figure 27: Cured EGDMA dogbone sample with PMMA-co-MAA filler

3.6 Incorporating GMA into the PMMA-co-MAA polymer

The process of adding Glycidyl methacrylate (GMA) takes place after the synthesis of the PMMA-co-MAA copolymer. Since the synthesized PMMA-co-MAA polymer comes as a solid block, it must first be grinded down into powder like consistency to aid in dissolving. This was achieved using glass mortar and pestle. The copolymer is then dissolved in toluene. The solution is added to the reactor along with

GMA, and the two are mixed thoroughly and evenly at a temperature of 70C for 24 hours. After the reaction period, the solution is drained from the reactor and left to dry.

To study the effect of GMA on the mechanical properties of the cross-linker when incorporated into the EGDMA mixture, different varying ratio of copolymer is created. Since only one GMA monomer binds to a single MAA monomer in the copolymer chain, varying the MAA to MMA ratio would alter the amount of GMA present in the polymer chain. The following figure shows how the GMA monomer binds with the PMMA-co-MAA copolymer:

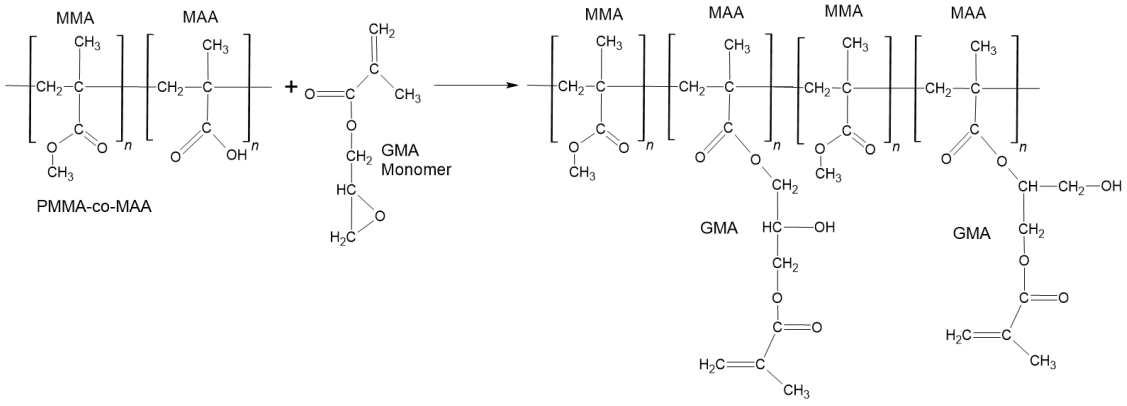

Figure 28: GMA combining with PMMA-co-MAA polymer

To prepare for this, five different ratios of monomers were created and used to synthesize the PMMA-co-MAA polymer. The ratio varies from 5:1 MMA to MAA to 1:1 MAA to MMA (wt/wt). The amount of initiator as well as MMA monomer is kept constants for all five batches, only changing the MAA monomer amount. Each ratio is created in two batches, one for use as a control and the other for adding GMA. Since only one GMA monomer can bind to one MAA monomer, amount of GMA needed is calculated based on the molar number of MAA in each batch. Table 3 shows the contents

and make up of each batch. Batches with the same number indicates similar MMA/MAA ratio, with the letter "G" in the batch name indicates that GMA is added to the polymer formulation, requiring a second stage of synthesis.

Table 3: Specification of each polymer batch

Batch	AIBN(g)	MMA(g)	MAA(g)	MAA/MMA Ratio	GMA (mols)	GMA (g)	Avg. Molar mass (g/mol)
B1	10	90	18	0.2	N/A	N/A	1937.678
B1G	10	90	18	0.2	0.209083517	29.72122198	2425.73
B2	10	90	36	0.4	N/A	N/A	2233.256
B2G	10	90	36	0.4	0.418167034	59.44244395	3209.36
B3	10	90	54	0.6	N/A	N/A	2528.834
B3G	10	90	54	0.6	0.627250552	89.16366593	3992.991
B4	10	90	72	0.8	N/A	N/A	2824.412
B4G	10	90	72	0.8	0.836334069	118.8848879	4776.621
B5	10	90	90	1	N/A	N/A	3119.99
B5G	10	90	90	1	1.045417586	148.6061099	5560.251

Since the number of moles of the polymer is determined by the molar amount of the AIBN initiator, molar mass is determined by dividing the total mass of all components added to the batch by the initiator molar amount.

To ensure consistency, every element is identical between each batch. For the first stage of synthesis, where MMA and MAA are combined to create PMMA-co-MAA polymer, the amount of solvent is kept at 900mL, with each batch being heated and mixed in the updated reactor for two hours after which the solution is removed and dried out. GMA included batches goes through a second stage of synthesis where the dried polymer is then redissolved into toluene, in which the solution is combined with the predetermined GMA amount and left to mix in the reactor for 24 hours. The drying

process is then repeated similar to the first stage. Reactor temperature and solvent amount is kept constant for both stages to ensure experiment consistency.

3.7 NMR Spectroscopy

Since the GMA and non-GMA copolymer are both physically similar, to confirm that GMA had successfully combined with the PMMA-co-MAA polymer, Nuclear Resonance Magnetic Spectroscopy (NMR) must be performed on the samples. NMR, specifically Hydrogen (H)-NMR, analyses hydrogen atom position within the molecule, with different atom positioning creating different and unique signatures in the spectrum. The MMA and MAA copolymer contain an epoxy ring located in the MAA monomer. These rings would open and bind with GMA, resulting in formation of the ester bonds between the GMA and MAA. H-NMR would identify these bonds

The copolymer contains both the MMA and MAA monomer within the chain. The MAA monomer contains a carboxyl functional group at its tail, which would bind to the GMA epoxy ring that opened during the polymer synthesis. The binding of GMA to the MAA would result in ester bond formation between the GMA and MAA, which would create unique signatures within the H-NMR spectrum. These signatures generally lie within the 3.2-4.2 ppm range. These signature differences between the GMA and non-GMA copolymer would confirm the formation of these ester bonds, which would verify that GMA had combined successfully to the copolymer.

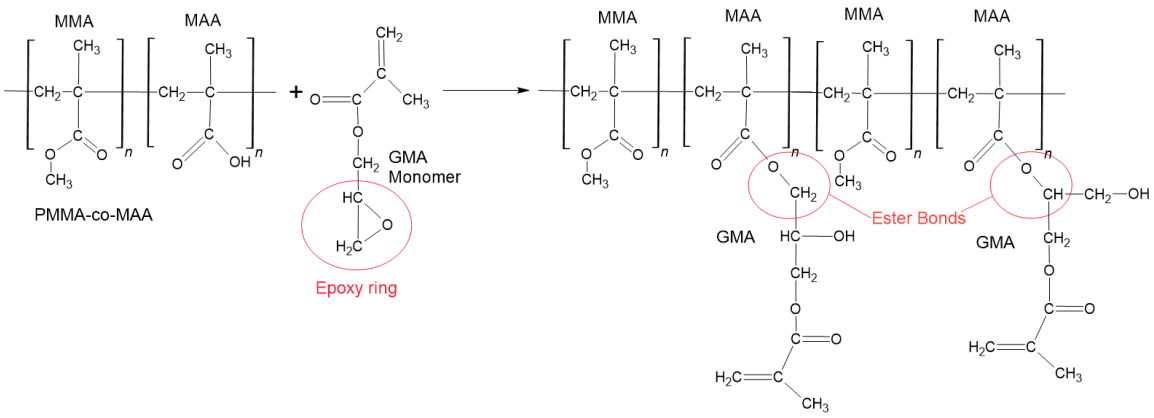

Figure 29: GMA forming ester bonds with MAA in the copolymer

To obtain the H-NMR spectrum, the sample must first be dissolved in a deuterated solvent, which are solvents with Hydrogen atom replaced with Deuterium to not interfere with the spectrum reading. This mixture is put into the NMR tube, which is inserted into the sample holder, shown in Figure 30.

Figure 30: NMR tube containing the sample held by the holder

The sample was scanned using the Oxford 400MHz NMR machine at the Stephenson Life Sciences Research Center to obtain NMR data, shown in Figure 31.

Figure 31: 400 MHz Oxford NMR Machine

The obtained data is then processed using Spinworks 4 software. To ensure accuracy, all the spectra are calibrated using the signal produced by the deuterated chloroform, used as a solvent during the prep phase for NMR reading. The chloroform produces a signal of 7.26ppm, which could be identified clearly on the spectra. All spectra's vertical scaling is set to be identical. Figure 32 shows the spectra from B1 to B3 compared against B1G to B3G.

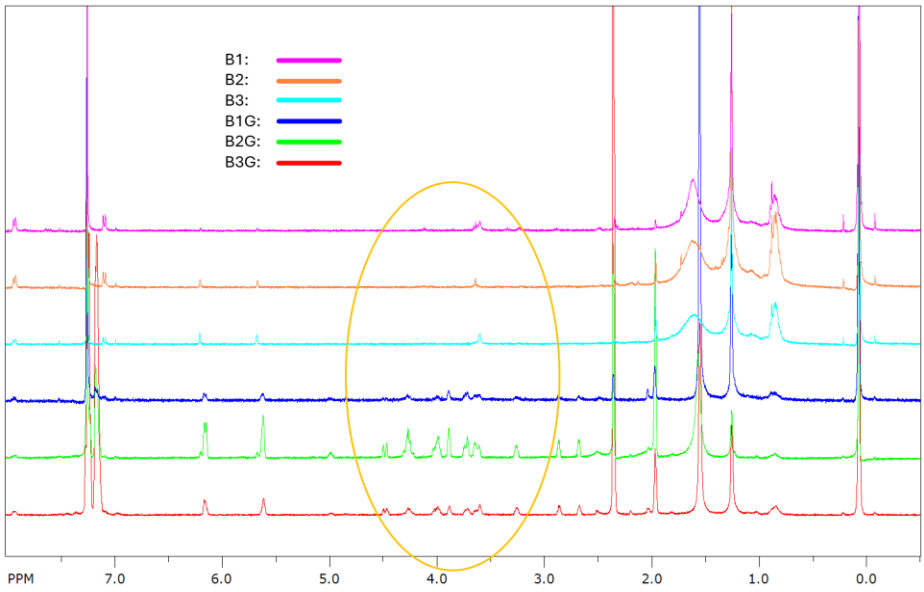

Figure 32:H-NMR spectra of B1 to B3 and B1G to B3G

In the batches containing GMA, signal difference between the two spectra could be seen between 3.2 to 4.2 ppm, as circled, indicating the formation of ester bonds connecting the GMA monomer to the MAA in the copolymer chain. Similar signal differences between 3.2 to 4.2 ppm could be seen when compared between B4, B5 and B4G, B5G, shown in the following figure.

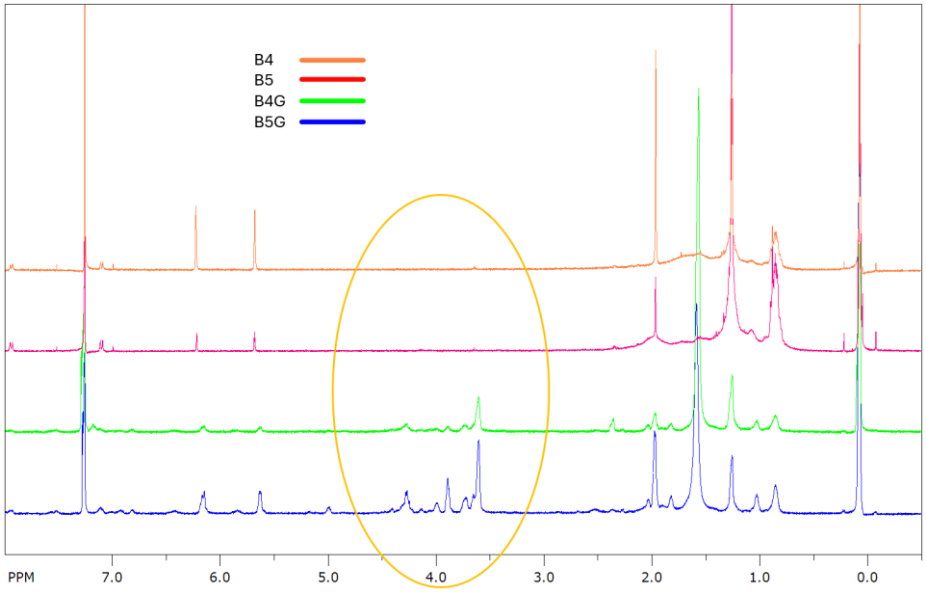

Figure 33: H-NMR Spectra Comparison between B4, B4G, B5, B5G

From the data gathered between all the spectra, it is confirmed that copolymer is modified with GMA successfully. After successful verification of the combination of GMA with the copolymer, dogbone manufacturing continues with the GMA containing batch. For consistency, the ratio of GMA copolymer and EGDMA is kept at 1:10 (wt/wt), similar to the ratio of the mixture with non-GMA copolymer. All synthesis processes of the GMA batch is repeated similarly to that of the non-GMA batch, with mixing time in the sonicator and curing time in the curing machine kept identical. The following figure shows the dogbone samples of one of the GMA batches.

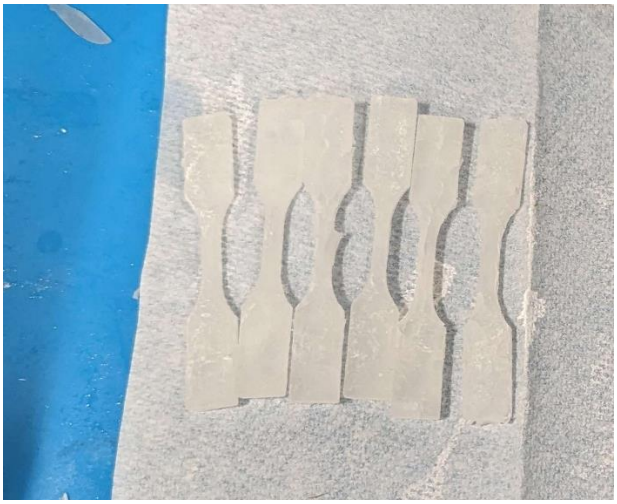

Figure 34: Dogbone synthesis from batch B3G

Some failures did occur to some of the dogbones, as seen from the image above. Some bones started to develop cracks after cooling down from curing but the number of failed dogbone is very minimal, only occurring once to batch B3G and twice to batch B4G.

Chapter 4: Tensile Testing

4.1 Acquiring Parts

Tensile testing is performed on the Instron 68Tm-50 Universal Tensile Testing machine, with a load capacity of 50kN. The Instron initially comes equipped with mechanical wedge action grips, which are manually tightened by hand and are designed to be suitable for high-strength materials.

Figure 35: Mechanical Wedge Action Grips, obtained from Instron catalogue

These jaws, however, are proven to be unsuitable for the material that is being tested. The jaws, having to be tighten manually, turns out to be the point that causes premature failure to the dogbone before tensile test could be performed. It is impossible for the operator to consistently control the clamp force of the jaws, which would cause either too high of a clamping force, which causes the dogbones to prematurely break at the clamping area, or too low, which causes slippage, invalidating the testing result. Because of this, in the initial testing batch, only 5 proper data points are gathered out of 15 testing samples, resulting in 66% failure rate. The second and third round of testing has a lower premature failure rate, but it is still around 50% to 60%, which is still too high. Most of the premature failures are caused by either slippage or the grip area breaking prematurely.

To tackle this, a different method of gripping the samples is considered, where the grip strength of the sample could be finely adjusted. The Instron tensile tester also comes with a set of high temperature pneumatic action grip (Model No. 2732-008)

which is capable of 1kN loading capacity. The grips are connected to pneumatic pull rods (Model No. 3119-306 and 3119-319) on which the air supply connection is located, as shown in Figure 36.

Figure 36: Pneumatic pull rods (image by Instron)

The automatic air control kit (Part No. 2701-065), shown in Figure 37, is used to control the opening and closing action of the grips. There are two problems with the pneumatic grips and the included accessories: the kit provides no control over the grip force and one of the pull rods doesn't have the correct adapter to install to the Instron frame.

Figure 37:Instron Automatic Air Control Kit (image by Instron)

During initial testing of the grip strength of the jaws, it is found that the pressure of the air supply provided in the lab, which is also used to power other pneumatic equipment, is too high. Other pneumatic equipment in the lab requires around 100 psi to operate properly, but using this pressure on the jaws would completely destroy the grip pads of the dog bone samples. A dogbone sample made from PLA is used to demonstrate the overpressure of the jaws, shown in the following figure.

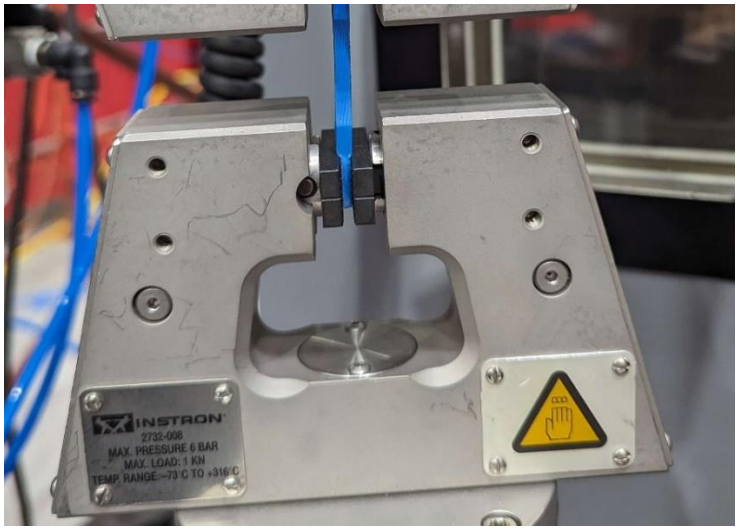

Figure 38: Dogbone grip destroyed by pneumatic jaw due to overpressure

To address this, a pressure regulator is added in the connection between the air control kit and the pull rods, allowing grip strength control of the jaws, shown in Figure 39. Different air pressures are tested ranging from 10 to 50 psi, with the air pressure of 20 psi found to be the best balance between providing the proper grip force as well as minimally damaging the dog bone grip pads, avoiding potential premature sample failure.

Figure 39: Pressure Regulator used to adjust grip strength of the jaws

As for the incompatibility between the pull rods and the Instron frame, the company does sell adapters, but those could not be obtained in a suitable time frame. Instead, an adapter is modeled using Solidworks and manufactured in-house using FDM 3D printing. The adapter model is displayed in Figure 40.

Figure 40: Pneumatic pull rod adapter

The part is printed out of polycarbonate filament, using the Bambulab X1C printer. Polycarbonate is selected due to its exceptional mechanical properties and its availability in the lab. To ensure that the part will hold up during operation, tensile simulation is performed using SolidWorks Simulation. Due to the relatively low pulling speed of the nature of tensile testing, for the simulation, static load sim is selected. A load of 100N is selected for simulation testing as it is double the highest load that was achieved during previous tensile tests. The following is the result of the simulations

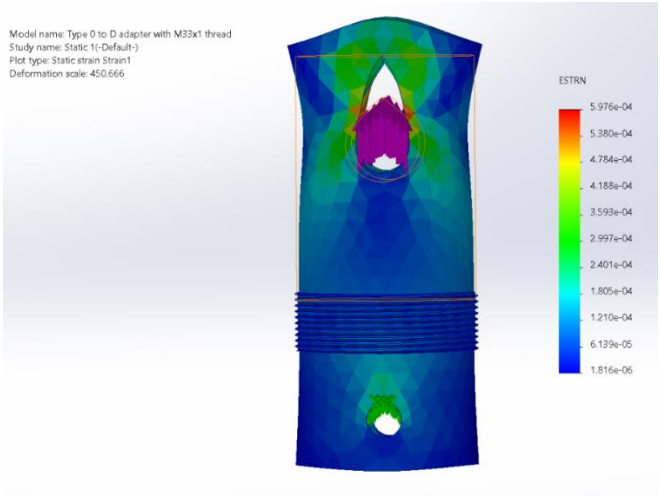

Figure 41: Equivalent Strain result from simulation

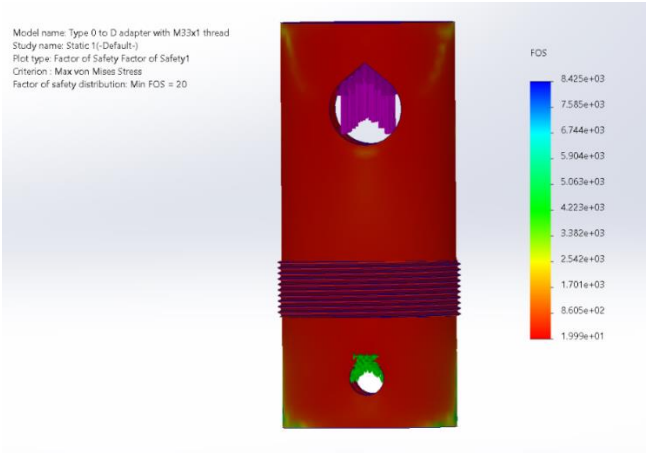

Figure 42: Factor of Safety result from simulation

The resulting simulation shows the minimum safety factor of 20 and the highest equivalent strain of 5.97 x 10^{-4}. Based on the simulation results, the highest equivalent strain the part is more than strong enough to sustain the load with minimal

deformation, therefore not affecting the test results. The part installation is shown in Figure 43.

Figure 43: Fabricated adapter connecting the pull rod to the Instron tester

4.2 Testing Result

Before tensile testing could begin, dimension measurements are taken in the gauge region of the dogbone to account for any skewness that could occur during the manufacturing process. Tensile tests are then performed on each batch five times to account for statistical significance. Each dogbone is pulled at a ramp rate of 0.002mm/min/min. The full tensile testing setup is shown in the following figure:

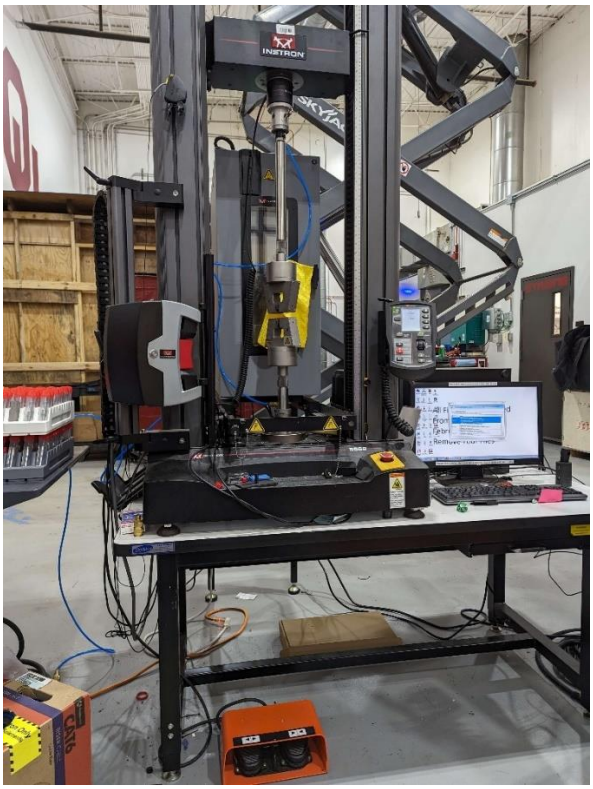

Figure 44: Full Tensile Testing Setup

All data is processed using Microsoft Excell. The following figure shows one of the engineering stress-strain curve from one sample in batch B4

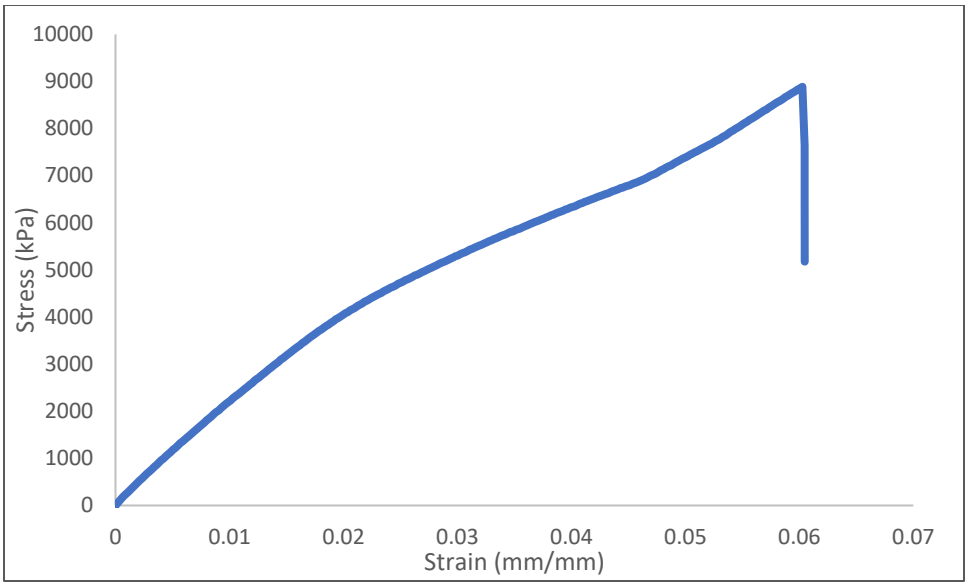

Figure 45: Stress-strain curve of sample 4 batch B4

Most of the sample stress-strain curves follow this curve profile, even between all batches. Based on the shape of the curve, as well as the lack of necking and deformation in broken samples, as shown in Figure 46, this material is identified to be brittle.

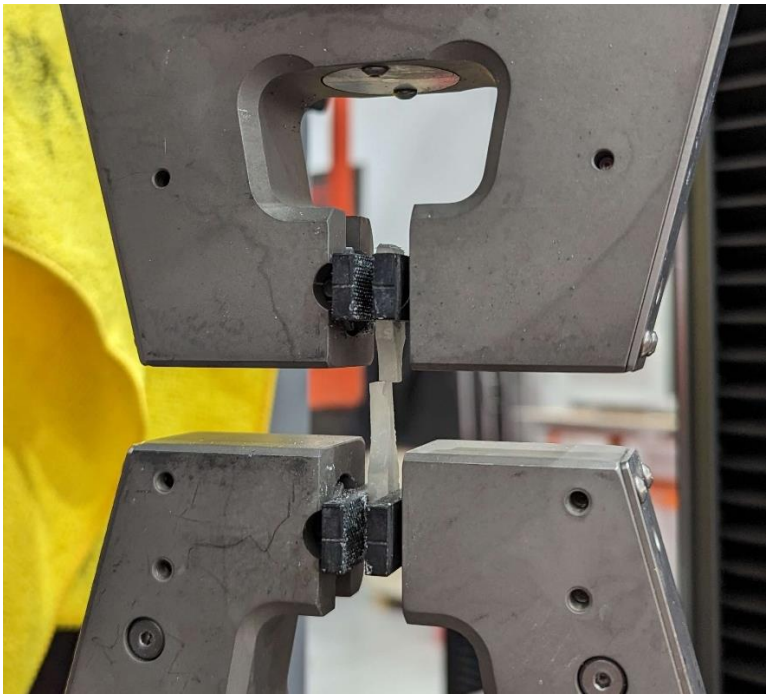

Figure 46: broken dogbone sample after tensile testing

Due to the nature of the shape of the stress-strain curve, the yield strength could not be identified easily. Instead, yield strength is identified at 0.2% proof stress, which represents the stress level at which a permanent strain of 0.2% remains in the material after unloading. This value is often used in place of material where no distinct yield strength point could be identified. The following graph shows the average yield strength of each batch identified at 0.2% proof stress.

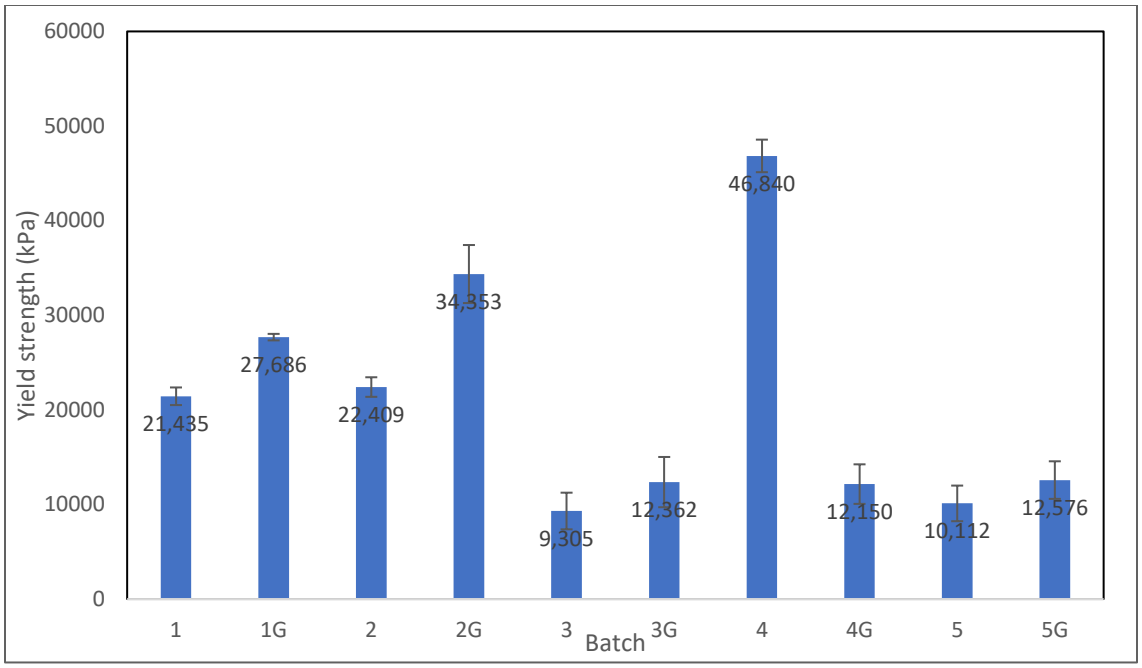

Figure 47: Average yield strength of each batch

Based on the data gathered, it seems that the molecular weight of the polymer in non-GMA batches does increase the yield strength of the material up to a point. Minor incremental changes could be seen between batches 1, 2 and 3, with a 90% yield strength increment between batches 2 and 3. Batches 4 and 5, however, do not show any significant change in yield strength compared to batch 3. When compared between GMA and non-GMA batches, the addition of GMA shows an increase in yield strength in all batches except for batch 1, with the highest increase shown in batch 2 with an almost 300% gain in yield strength. Again, higher molecular weight shows diminishing returns. Despite that, batches with higher molecular weight are shown to have lower standard deviation, as seen in batch 4G, 5, and 5G. This shows that batches with higher molecular weight tend to have much higher consistency compared to batches with lower molecular weight.

Figure 48 shows the ultimate tensile stress (UTS) of each batch, with the error bars describing the standard deviation that occurred within the batch.

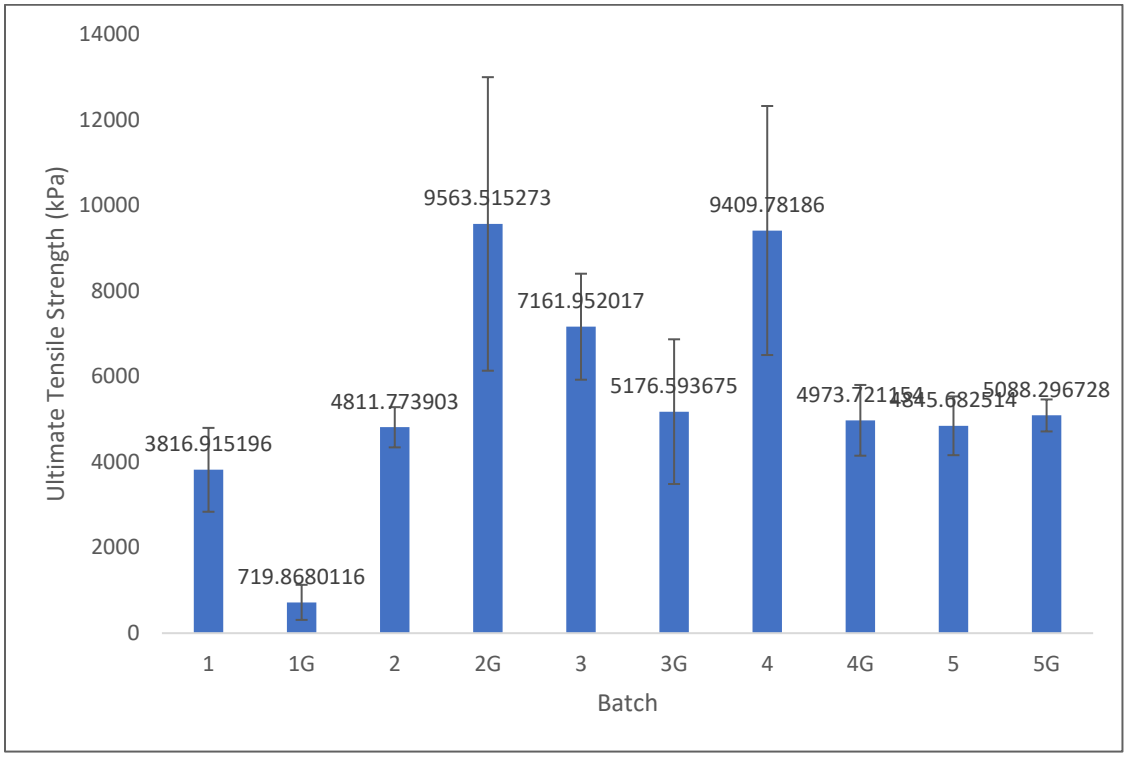

Figure 48: Ultimate tensile strength between each batch

Between non-GMA batches, there is some correlation between UTS and molecular weight. All batches between 1 and 4 show an increase in UTS at each higher molecular weight, with batch 5 being an outlier, showing around half the UTS of batch 4, roughly the same as batch 2. When comparing GMA to non-GMA batches, there seems to be no correlation between the addition of GMA to UTS, as the effects are all over the place. Similar to yield strength, higher molecular weight does also provide a more consistent result, with batch 4G, 5, and 5G having smaller standard deviation for its UTS value compared to the other batches.

Figure 49 shows the average Young's modulus of elasticity (YM) comparing between all batches

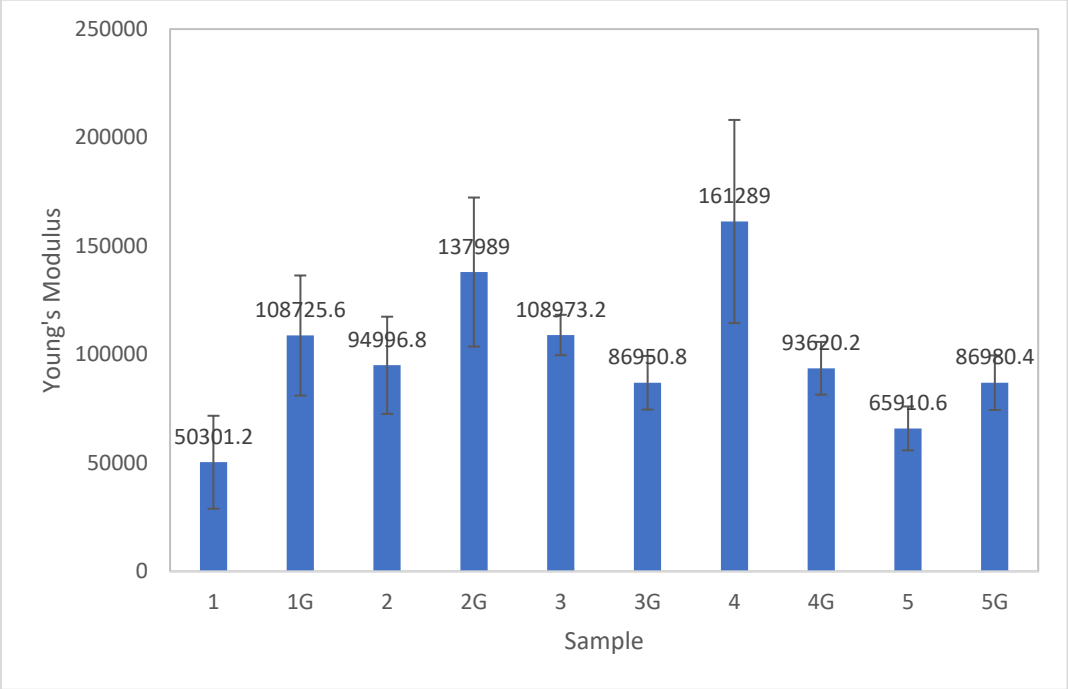

Figure 49: Average Young's modulus of all batches

The same trend is repeated following the same pattern as UTS between the non-GMA batches. The Young's Modulus increase as molecular weight gets higher up to batch 4, with an average increase of 20% for each batch increment. Batch 5, being an outlier of the trend, has lower YM compared to its immediate lower molecular weight batch. Between GMA and non-GMA batches shows inconsistent correlation when GMA is added. Batch 1, 2, and 5 benefits from an increase in UTS ranging from 30 to 100%, with the highest increment occurring between batch 1 and 1G.

Other than tensile properties, the gauge dimensions of the dogbone samples for each batch are also recorded. Using this collected data, as well as the original mold

dimensions, it is possible to quantify the shrinkage that occurred for each batch. Figure 50 shows the average depth of each batch:

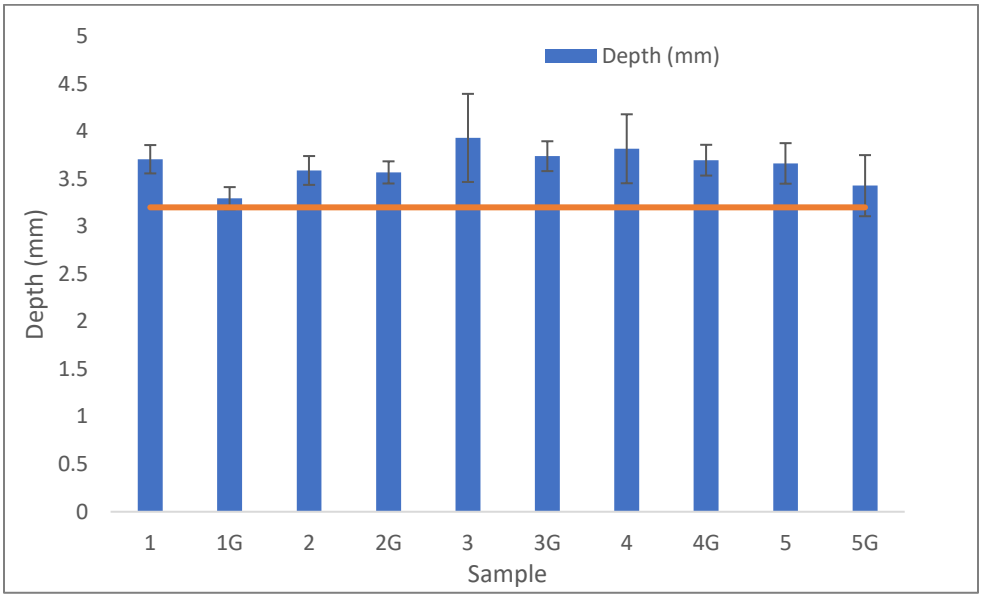

Figure 50: Average Depth of each batch

All of the average depth of each batch exceeds the depth of the dogbone specification. This could be due to the inconsistency in the amount of material poured into the mold because of the design of the mold being open top. As a result, the depth dimension could not be used to quantify shrinkage rate. The same problem would not occur when using the width measurement of the gauge length since the sides of the

Figure 51 shows the average width of the gauge area of each batch compared to the mold dimension.

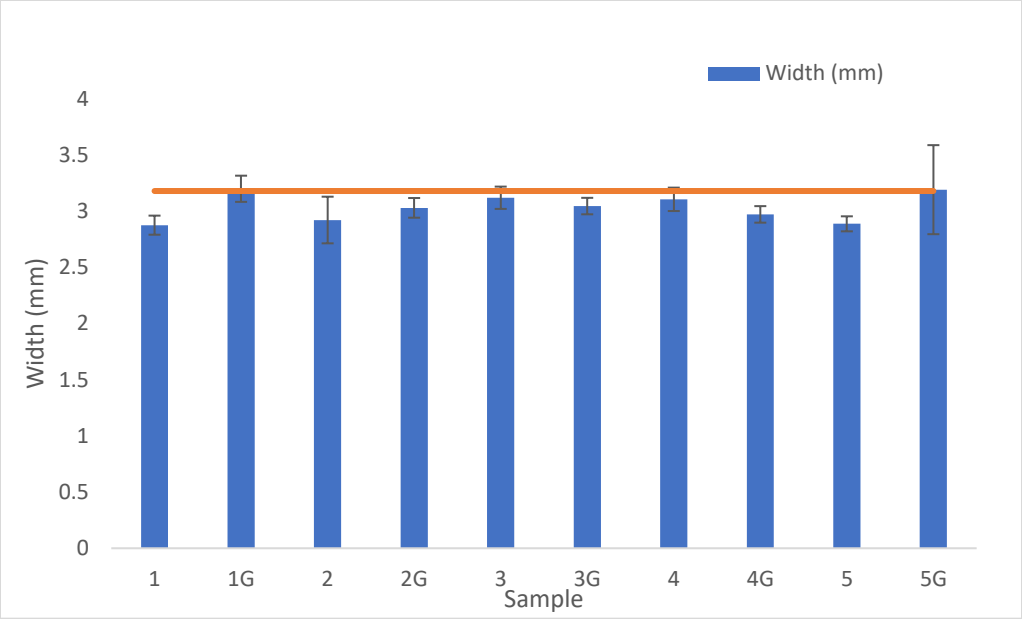

Figure 51: Average width of each batch compared to mold dimension

Based on the compiled data, most batch experienced shrinkage, with the exception being batch 1G and 5G. The following table shows the average linear shrinkage rate calculated from each batch

Table 4: Average linear shrinkage rate of each batch

Batch	Linear Shrinkage Rate (%)
1	10.57
1G	-0.63
2	8.83
2G	4.95
3	1.92
3G	4.40
4	2.38
4G	7.00
5	10.11
5G	-0.38

The highest linear shrinkage rate occurred in batch 1 with an average shrink rate of almost 10.6%, followed by batch 5 with an average of 10.11%. Batch 1G and 5G shows negative shrinkage rate, which indicates that the sample, on average, increase in size. The expanding rate is very minor, at less than 1% for both batches. Comparing the standard deviation between the two outliers, batch 5 has a larger deviation. Since the batches are made in numerical order, with batch 5G being the last, the slight expansion could be due to gradual breakdown of the silicone mold. This breakdown could be caused by basic wear and tear accelerated by heat exposure from the exothermic process of the monomer cross-linking.

Chapter 5: Conclusion and Future Work

5.1 Conclusion

This thesis has demonstrated the ability to create an EGDMA based dental resin that would allow the use of 3D printing to create a more customizable dental prosthesis. This work successfully experimented and found a photoinitiator that would react with EGDMA, allowing the monomer to react with UV light with wavelength compatible with SLA printers. This ability to work with SLA printers allows higher degree of customization, permitting the creation of more tailored prosthesis.

In addition to this, PMMA based filling material is synthesized, using as a filler to the cross-linked EGDMA, creating a composite material with better stability compared to pure EGDMA. The synthesis of this material is achieved along with improvements to the method as well as the synthesis equipment, creating a more reliable and streamlined method of producing the copolymer. By varying the molecular weight, ratio as well as the addition of GMA on the copolymer, different effects could be observed on the mechanical properties of the material as a whole. Higher molecular weight copolymer improves the Modulus of Elasticity as well as UTS of the composite. The addition of GMA shows mixed results, with batch B2G, having 0.4 MAA:MMA ratio showing the best improvement in term of mechanical properties. The addition of GMA shows a 45% increase in Young's Modulus, 66% increase in Yield Strength, and 49% increase in Ultimate Tensile Strength for B2G specifically. This improvement shows that the ratio of B2G has the best mechanical properties out of all GMA batches.

5.2 Future Work

There are some elements that presents an opportunity for refinement. The process of synthesizing the copolymer could be further optimized by eliminating some elements, such as removing the drying and redissolving stage before adding GMA into the batch. This would significantly reduce the manufacturing time of the batch as well as reduce the copolymer's exposure to moisture. Also, more testing could be done with different copolymers to EGDMA concentration to find the optimal ratio for both stability and improvement in mechanical properties. Furthermore, additional elements could be added to the EGDMA-copolymer mixture to make it more compatible with SLA printers on the market, such as elements to prevent the splitting of the copolymer from the EGDMA mixture, improving suspension stability to keep even distribution of the mixture during print.

With these improvements, the technology could be further improved to be used to make 3D print dental prosthesis, allowing a more personalized prosthesis fitment, creating better variety options compared to contemporary methods[16].

Bibliography

[1] F. Bernardini *et al.*, "Beeswax as Dental Filling on a Neolithic Human Tooth," *PLoS ONE*, vol. 7, no. 9, p. e44904, Sep. 2012, doi: 10.1371/journal.pone.0044904.

[2] "George Washington's Teeth | George Washington's Mount Vernon." Accessed: Jul. 05, 2025. [Online]. Available: https://www.mountvernon.org/george-washington/health/washingtons-teeth

[3] D. Rokaya, V. Srimaneepong, J. Sapkota, J. Qin, K. Siraleartmukul, and V. Siriwongrungson, "Polymeric materials and films in dentistry: An overview," *J. Adv. Res.*, vol. 14, pp. 25–34, Nov. 2018, doi: 10.1016/j.jare.2018.05.001.

[4] K. J. Anusavice DMD, *Phillips' Science of Dental Materials - E-Book: Phillips' Science of Dental Materials - E-Book*, 12th ed. Chantilly: Elsevier - Health Sciences Division, 2012.

[5] R. J. Young and P. A. Lovell, *Introduction to polymers*, 3rd ed. Boca Raton: CRC press, 2011.

[6] "Nondestructive Evaluation Physics : Materials." Accessed: Jul. 09, 2025. [Online]. Available: https://www.nde-ed.org/Physics/Materials/Structure/polymer.xhtml

[7] W. J. Tuckfield and H. K. Worner, "Acrylic resins in dentistry: obturators, flexible or rigid facial restorations, splints and artificial teeth," *Aust J Dent*, vol. 49, pp. 10–28, 1945.

[8] 3D PrintingGuides26 minutes read, "SLA vs. DLP vs. MSLA vs. LCD: Guide to Resin 3D Printers," Formlabs. Accessed: Jul. 11, 2025. [Online]. Available: https://formlabs.com/blog/resin-3d-printer-comparison-sla-vs-dlp/

[9] J. V. Crivello and E. Reichmanis, "Photopolymer Materials and Processes for Advanced Technologies," *Chem. Mater.*, vol. 26, no. 1, pp. 533–548, Jan. 2014, doi: 10.1021/cm402262g.

[10] L. W. McKeen, "Introduction to Creep, Polymers, Plastics and Elastomers," in *The Effect of Creep and Other Time Related Factors on Plastics and Elastomers*, Elsevier, 2015, pp. 1–41. doi: 10.1016/B978-0-323-35313-7.00001-8.

[11] T. Lodge and P. C. Hiemenz, *Polymer chemistry*, Third edition. Boca Raton: CRC Press, 2020.

[12] L. Ling, T. Lai, and R. Malyala, "Mechanical Properties and Degree of Conversion of a Novel 3D-Printing Model Resin," *Polymers*, vol. 16, no. 24, p. 3562, Jan. 2024, doi: 10.3390/polym16243562.

[13] L. Musanje, J. L. Ferracane, and R. L. Sakaguchi, "Determination of the optimal photoinitiator concentration in dental composites based on essential material properties," *Dent. Mater.*, vol. 25, no. 8, pp. 994–1000, Aug. 2009, doi: 10.1016/j.dental.2009.02.010.

[14] K. Wang, B. Li, K. Ni, B. Li, and Z. Wang, "Optimal photoinitiator concentration for light-cured dental resins," *Polym. Test.*, vol. 94, p. 107039, Feb. 2021, doi: 10.1016/j.polymertesting.2020.107039.

[15] K. Hata, H. Ikeda, Y. Nagamatsu, C. Masaki, R. Hosokawa, and H. Shimizu, "Development of Dental Poly(methyl methacrylate)-Based Resin for Stereolithography Additive Manufacturing," *Polymers*, vol. 13, no. 24, p. 4435, Dec. 2021, doi: 10.3390/polym13244435.

[16] F. Rezaie *et al.*, “3D Printing of Dental Prostheses: Current and Emerging Applications,” *J. Compos. Sci.*, vol. 7, no. 2, p. 80, Feb. 2023, doi: 10.3390/jcs7020080.